İSTANBUL TECHNICAL UNIVERSITY ★ INSTITUTE OF SCIENCE AND TECHNOLOGY

THE TOXIC EFFECTS OF XENOESTROGENS ON CYTOSKELETAL PROTEINS

M.Sc. Thesis by

Eyser KILIÇ, B.Sc.

Department : Advanced Technologies in Engineering

Programme: Molecular Biology - Genetics & Biotechnology

JUNE 2005

İSTANBUL TECHNICAL UNIVERSITY ★ INSTITUTE OF SCIENCE AND TECHNOLOGY

THE TOXIC EFFECTS OF XENOESTROGENS ON CYTOSKELETAL PROTEINS

M.Sc. Thesis by

Eyser KILIÇ, B.Sc.

(707021007)

Date of submission : 9 May 2005

Date of defence examination: 30 May 2005

Supervisor (Chairman): Assist. Prof. Dr. Arzu KARABAY KORKMAZ

Members of the Examining Committee Prof. Dr. Turgut ULUTİN (İÜ)

Assist. Prof. Dr. Cenk SELÇUKİ (İTÜ)

JUNE 2005

ACKNOWLEDGEMENTS

I would like to thank Assist. Prof. Dr. Arzu Karabay Korkmaz, my advisor, for providing invaluable guidance, advice, criticism, and encouragement.

I would like to thank Ceren Eke Koyuncu for being the best lab-mate and providing me morale support at any time either inside or outside the lab. This study was more enjoyable and efficient with her for me.

I would like to thank my friends; Hilal Yazıcı, M. Hale Öztürk, Şirin Korulu, Volkan Demir for their morale support and deepest friendship.

I would like to thank Physics Department of Istanbul Technical University, Demet Kaya and Kerem Teralı for providing technical support during Fluorescence Spectroscopy experiments.

I would like to thank Histology and Embryology Department of Istanbul Medical Faculty, Assoc. Prof. Dr. Seyhun Solakoğlu, Ebru Karabulut, and Fadime Aktar for providing technical support during Electron Microscopy experiments.

I would like to thank Molecular Biology and Genetics Department of Istanbul Technical University for their encouragement and support they have provided.

I also would like to mention that this study was supported by Turkish State Planning Organization.

Finally, I would like to send my special thanks to my family and Serkan for their strength, motivation, confidence, and morale support to do my best in my education and career.

May 2005 Eyser KILIÇ

TABLE OF CONTENTS

ABBREVIATIONS

ADP	: Adenosine Diphosphate
APS	: Amonium Persulfate
ATP	: Adenosine Triphosphate
BADGE	: BPA diglycidylether
Bis-GMA	: BPA diglycidyl methacrylate
BPA	: Bisphenol A
BSA	: Bovine serum albumin
C_c	: Critical Concentration
CMTC	: Cytoplasmic Microtubule Complex
CNS	: Central Nervous System
DES	: Diethylstilbestrol
DMSO	: Dimethylsulfoxide
DNA	: Deoxyribonucleic acid
DTT	: Dithiothreitol
E_2	: 17β-Estradiol
EDC	: Endocrine Disrupting Chemicals
EGTA	: Ethyleneglycol bisamino tetraacetic acid
ER	: Estrogen Receptor
GH	: Growth Hormone
GDP	: Guanosine Diphosphate
GTP	: Guanosine Triphosphate
kD	: Kilo Dalton
MAPs	: Microtubule-associated proteins
mRNA	: Messenger Ribonucleic Acid
MT	: Microtubule
MTOC	: Microtubule Organizing Center
NO	: Nitric Oxide
PCR	: Polymerase Chain Reaction
P_i	: Inorganic Phosphate
PMSF	: Phenyl Methyl Sulfonyl Fluoride
pTb	: Purified Tubulin
RT	: Room Temperature
SDS	: Sodium Dodecyl Sulfate
SDS-PAGE	: Sodium Dodecyl Sulfate Polyacrylamide Gel Electrophoresis
spTb	: Semi-purified Tubulin
TEM	: Transmission Electron Microscope
TEMED	: Tetramethylene diamine
TMT	: Taxol-stabilized Microtubules
TNF	: Tumor Necrosis Factor
UV	: Ultraviolet

LIST OF TABLES

LIST OF FIGURES

KSENOÖSTROJENLERİN HÜCRE İSKELET PROTEİNLERİ ÜZERİNDEKİ TOKSİK ETKİLERİ

ÖZET

Ksenoöstrojenler endojen hormonları taklit edebilir ya da endokrin prosesleri etkileyebilirler ve endokrin bozucu olarak adlandırılırlar. Ksenoöstrojenlerin yan etkileri çok sayıda gelişimsel anomalileri kapsar. Bu çalışmanın konusu olan Bisphenol A (BPA) bir endokrin bozucudur. BPA polikarbonat, epoksi ve diğer rezinlerin monomeridir. Polikarbonatlar geri dönüşümlü içecek kapları, biberonlar, plastik yiyecek eşyaları ve plastik depolama kapları gibi çeşitli tüketici ürünlerinin yapımında kullanılır. Epoksi gıda endüstrisinde konserve kutuların kaplamalarında ve dişçilikte güçlendirici materyallerde kullanılmaktadır. BPA bu kaynaklardan açığa çıkarak insanlar ve doğal hayatın maruz kaldığı çevresel bir toksik ajan oluşturur. BPA reprodüktif sistem anomalilerine neden olmaktadır ve çeşitli sistemler üzerinde de birçok yan etkisi bulunmaktadır. BPA'nın hücrede iğ mikrotubulleri, mikrotubul-ilişkili proteinleri, kinetokorları, sentromer, sentrozom ve sentriolleri ve DNA'yı hedef aldığı önerilmektedir.

Hücre iskeleti hücreye düzgün şekil ve uygun yapı veren bir filament ağıdır. Ökaryotik hücrelerde üç çeşit filament bulunmaktadır, ara filamentler, mikrotubuller ve aktin filamentleri. Mikrotubul polimerizasyon ve depolymerizasyon dinamikleri gerek bölünen gerekse bölünmeyen hücrelerde normal hücresel fonksiyonun ve morfolojilerin sağlanmasında çok önemli rol oynarlar.

Bu çalışmada BPA'nın mikrotubuller üzerindeki etkileri araştırıldı. Mikrotubul proteinleri taze dana beyninden iki devir polimerizasyon ve depolimerizasyon metoduyla elde edildi. BPA'nın mikrotubul polimerizasyon ve depolimerizasyon özellikleri üzerindeki etkilerini incelemek amacıyla sedimentasyon deneyleri, floresans spektroskopi ve elektron mikroskopi metodları gerçekleştirildi.

BPA mikrotubul polimerizasyonunu inhibe etti ve taksolle-stabilize edilmiş mikrotubulleri depolimerize etti. Elektron mikrograflarında BPA'nın depolimerizasyon ve çözülmeyle tutarlı, gevşek ve spiral gibi farklı mikrotubul yapılarına neden olduğu gözlendi. Sonuçlar ayrıca BPA'nın mikrotubuller üzerindeki etkisini mikrotubul-ilişkili proteinler aracılığıyla gösterdiğini öne sürmektedir.

THE TOXIC EFFECTS OF XENOESTROGENS ON CYTOSKELETAL PROTEINS

SUMMARY

Xenoestrogens can mimic endogenous hormones or interfere with endocrine processes hence they are called "endocrine disrupters". Adverse effects of xenoestrogens include a number of developmental abnormalities. Bisphenol A (BPA) which is the subject of this study is an endocrine disrupter. BPA is monomers of polycarbonate, epoxy and other resins. Polycarbonates are used in a variety of consumer products such as returnable beverage containers, infant feeding bottles, plastic dinnerware, and plastic storage containers. Epoxy is used in coating of cans in the food industry and in restorative materials used in dentistry. BPA is an environmental toxicant since it can be released from these sources, resulting in human and wildlife exposure. BPA causes reproductive system abnormalities and it has also several adverse effects on various systems such as skin, central nervous system and immune system. BPA is proposed to target spindle microtubules, microtubule-associated proteins, kinetochores and centromeres, centrioles and centrosomes, as well as DNA in the cell.

The cytoskeleton is a network of filaments in cells that gives correct shape and proper structure to them. Three types of cytoskeletal filaments are common in eukaryotic cells, intermediate filaments, microtubules and microfilaments (actin filaments). Microtubule assembly and disassembly dynamics are crucial for both dividing and non-dividing cells in maintaining normal cellular function and morphologies.

In this study, the effects of BPA on microtubules were investigated. Microtubule proteins were obtained from fresh bovine brain by two cycles of polymerization and depolymerization method. To analyze the effects of BPA on microtubule assembly and disassembly properties, sedimentation assays, fluorescence spectroscopy and electron microscopy techniques were used.

The experimental results indicated that BPA inhibited microtubule polymerization and depolymerized taxol-stabilized microtubules. Electron micrographs showed that BPA caused changes in microtubule structures such as spiral, relaxed microtubules, consistent with depolymerization and disintegration. Results also suggested that BPA may show its effects on microtubules through microtubule-associated proteins.

1. INTRODUCTION

1.1. CYTOSKELETON

The cytoskeleton is a network of filaments in cells that gives correct shape and proper structure to them. Many of the cells also have to be able to change their shape and move to other places. All cells have to rearrange their internal components as they grow, divide and adapt to changing circumstances. The cytoskeleton pulls the chromosomes apart at mitosis and splits the dividing cell into two. It drives and guides the intracellular traffic of organelles and materials inside the cell and also supports the fragile plasma membrane. The cytoskeleton enables some cells, such as sperm, to swim and others, such as fibroblasts to crawl across surfaces and provides the machinery for the muscle cell contraction and extension of axons and dendrites in neurons [1].

Three types of cytoskeletal filaments are common in eukaryotic cells, intermediate filaments, microtubules and actin filaments. Intermediate filaments are rope-like fibers and they have a diameter about 10 nm. These filaments provide mechanical strength and resistance to shear stresses. Microtubules are long, hollow cylindirical structures made of tubulin subunits. The diameter of a microtubule is 25 nm. Microtubules determine the position of organelles and direct intracellular transport. Actin filaments are also known as microfilaments. They are two-stranded helical polymers and have a diameter about 5-9 nm. They appear as flexible structures and are organized into linear bundles, two dimensional networks and three dimensional gels. Actin filaments are dispersed throughout the cell and mostly found in the cortex, just beneath the plasma membrane. Intermediate filaments are made of elongated and fibrous subunits, whereas actin filaments and microtubules are made of compact and globular subunits (actin subunits for actin filaments, tubulin subunits for microtubules) [1, 2, 3].

A large number of accessory proteins link these filaments to each other and to other cell components. These are called “motor proteins” and they move membrane-bound

organelles and vesicles along the filaments or move the filaments themselves. These proteins use energy from ATP to walk or slide along a microtubule or a microfilament [1].

The size of the cytoskeletal protein molecules is about a few nanometers. Large number of these small subunits assemble and build large structures. The subunits are small, so they can easily diffuse in cytoplasm, but the assembled filaments cannot. The cytoskeletal polymers are held together by hydrophobic interactions and weak noncovalent bonds, so assembly and disassembly of them occur rapidly. They are built of multiple protofilaments that are made of subunits joined end to end, and these protofilaments associate with each other laterally to form the hollow microtubule structure [1, 3].

For a large filament to form, small subunits have to assemble into an initial nucleus, and then this is stabilized by many subunit-subunit contacts and can elongate rapidly by addition of more subunits. The process of the formation of the nucleus is called "nucleation". If we initiate the polymerization in a test tube that contains pure protein subunits, an initial lag phase occurs and no filaments can be observed. During this lag phase, nuclei assemble and rapid filament elongation phase follows it where subunits add to the ends of the nucleated filaments. The system approaches to a steady state where the rate of addition of new subunits are balanced to the rate of dissociation of subunits. At this point the concentration of free subunits in the solution is called "critical concentration" (C_c) [1]. The more dynamic end of the filament where both growth and shrinkage are fast is called the plus end, and the other end is called the minus end [1, 2].

1.1.1. ACTIN

Actin is the most abundant intracellular protein in eukaryotic cells. It is encoded by a large, highly conserved gene family and is a moderate-sized protein that consists of 375 residues [1, 4]. Actin filaments are composed of monomeric actin subunits that are single globular polypeptide chains [5]. A globular monomer is called "G-actin" and a filamentous polymer is called "F-actin" which is a linear chain of G-actin subunits [2]. Each actin subunit has a binding site for ATP, and actin subunits assemble head to tail to generate filaments with a structural polarity [5]. Also, each actin molecule contains a Mg^{+2} ion complexed with either ATP or ADP. When ATP

or ADP is bound to G-actin, it affects the conformation of the molecule. Without a bound nucleotide, G-actin denatures very quickly. The addition of ions (Mg^{+2}, K^{+}, or Na^{+}) to a solution of G-actin induces the polymerization of G-actin subunits to F-actin filaments. This is also reversible, when the ionic concentration is lowered F-actin depolymerizes to G-actin [2, 6].

The polymerization of actin filaments occurs in three phases (Figure 1.1). The first phase is called "nucleation phase" in which G-actin aggregates into short, unstable oligomers and then, these oligomers form a stable nucleus. In elongation phase, the filament elongates by the addition of actin monomers to both of its ends. The third phase is called "steady state" where there is no net change in the total mass of filaments. Once the steady state phase is reached, the equilibrium concentration in the pool of unassembled subunits is called the critical concentration (C_c). Above this value, G-actin polymerizes in a solution [1, 2, 4]. Accessory proteins are not required for polymerization *in vivo*. Also hydrolysis of ATP to ADP and P_i affect the polymerization kinetics but is not necessary for polymerization to occur [1]. On actin filaments, the ATP-binding site points towards the minus end [5]. Hence, all subunits have the same polarity. The rates of monomer addition to the ends of actin filaments differ because of the polarity. In the (+) end, elongation is five to ten times faster than the (–) end. This difference is caused by a difference in C_c values at the two ends [1, 2].

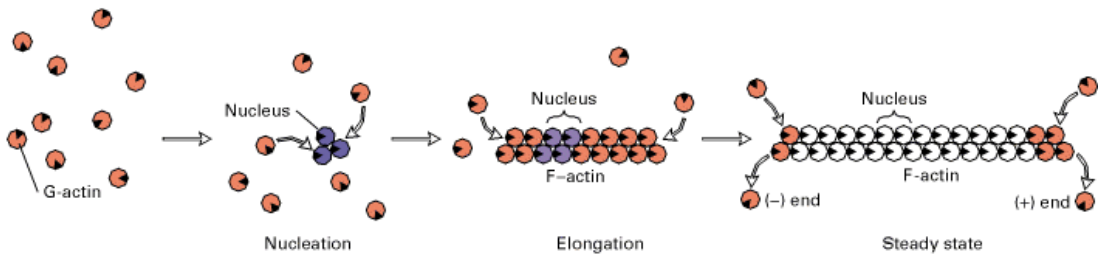

Figure 1.1. The three phases of G-actin polymerization in vitro [1].

The actin filament consists of two parallel protofilaments that twist around each other in a right-handed helix. In a living cell, actin filaments are cross-linked and bundled together by accessory proteins [5]. Actin filaments are arranged as bundles and networks in a cell, where organization of actin filaments are different depending

on the type of the cell. In bundles the actin filaments are closely packed in parallel arrays, whereas in a network they crisscross and are loosely packed. In bundles and networks, the actin filaments are held together by actin cross-linking proteins [1, 2, 6].

The actin cytoskeleton powers the cell migration. It controls the shape of the cell because the actin cytoskeleton is so big that it can easily change cell morphology by assembling or disassembling itself. Also, cell shape is dependent on membrane-microfilament binding proteins that connect the filaments to the membrane. The richest area of actin filaments in a cell lies in the cortex, just beneath the plasma membrane. Microvilli and filopodia are membrane projections that are supported by internal actin bundles [4, 7].

Several actin-binding proteins are involved in the regulation of actin polymerization in cells [1, 6]. Thymosin β4 inhibits the actin assembly whereas profilin promotes the assembly. Some proteins control the lengths of actin filaments by severing them. They bind to actin filaments and break them into shorter fragments. Cofilin, gelsolin, severin are examples to these proteins [7, 8]. Also actin-capping proteins stabilize actin filaments. They bind to the ends of actin filaments and prevents the addition or loss of actin subunits from the ends where they bind. CapZ and tropomodulin are the examples of these proteins. Such capped actin filaments are needed in places where the organization of the cytoskeleton is not changing, as in muscle sarcomere or in the erythrocyte membrane. The severing and capping proteins are regulated by several signaling pathways [1].

Actin polymerization and depolymerization create forces that produce several types of movement, such as the acrosome reaction of an echinoderm sperm cell, movement of intracellular pathogens and cell locomotion [1].

1.1.1.1. Myosin

Myosin is an ATPase that moves along the actin filaments and hydrolyses ATP [1]. Myosin is a motor protein as it converts chemical energy into mechanical energy [9].

Thirteen members of the myosin gene family have been identified. Myosin I and Myosin II are the most abundant and are present in nearly all eukaryotic cells. The specific activities of myosins differ, but they all function as motor proteins [1, 9].

All myosins are composed of one or two heavy chains and several light chains (Figure 1.2). The globular head domain contains actin- and ATP- binding sites, and it is responsible for generating force. The head domain is the most conserved region. Next to the head domain, α- helical neck region lies and is associated with the light chains. It regulates the activity of the head domain. The tail domain contains the binding sites which determine the specific activities of a particular myosin in the cell [9, 10]. Myosin ATPase activity is actin-activated. In the absence of actin, myosin slowly converts ATP into ADP and P_i in solutions. When myosin is complexed with actin, the rate of myosin ATPase activity is four to five times faster than in the absence of actin [11].

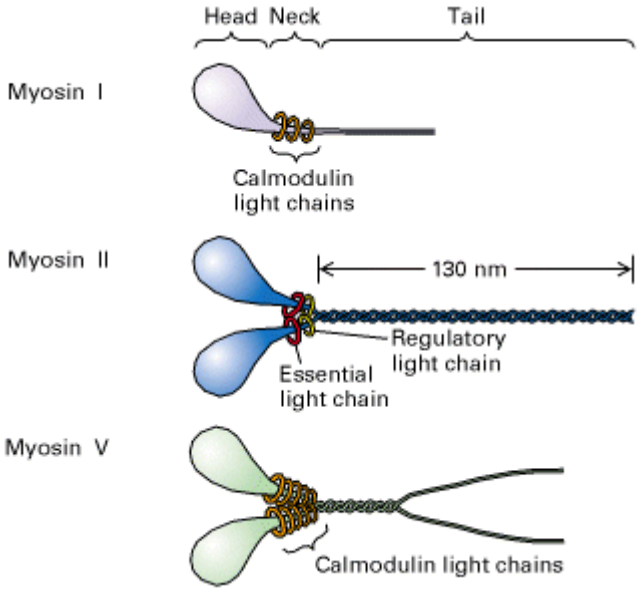

Figure 1.2. Structure of various myosin molecules [1].

Myosin heads slide or walk along actin filaments. This movement is caused by the myosin head walking toward the (+) end of the filament [11].

In muscle, actin and myosin associate in a complex called acto-myosin and they exploit to contract the muscle. According to the sliding-filament model of contraction in muscle, ATP-dependent interactions between thick filaments (myosin) and thin filaments (actin) generate a force which causes thin filaments to slide past thick filaments. The force is generated by the myosin heads of thick filaments and the two filament systems overlap. Some conformational changes occur and these cause the myosin heads to walk along the actin filament. Contraction of an

intact muscle results from the activity of myosin heads on a single thick filament, amplified by the thick filaments in a sarcomere and sarcomeres in a muscle fiber [12, 13].

In nonmuscle cells, interactions of actin filaments with various myosins are important in such cellular functions as support, cytokinesis and transport. In cell adhesion, actin filaments and myosin II form contractile bundles as in sarcomeres. Also during cytokinesis, actin-myosin II bundle forms and pinches the dividing cell into two halves. Myosin I and myosin V power intracellular translocation of some vesicles along actin filaments [1, 14].

1.1.2. MICROTUBULES

Microtubules are responsible for various cell movements such as beating of cilia and flagella, the transport of membrane vesicles in the cytoplasm, the alignment and separation of chromosomes during meiosis and mitosis, and, in some protists, the capture of prey by spiny extensions of the surface membrane. They all result from the polymerization and depolymerization of microtubules or the actions of microtubule motor proteins. Microtubules also promote the extension of the neuronal growth cone, so they direct the migration of nerve-cell axons [1, 15].

1.1.2.1. Microtubule Structure

Microtubules are formed from protein subunits of tubulin. Tubulin is a heterodimer formed from two related globular proteins called α-tubulin and β-tubulin [5]. Both of them have a molecular weight of 55 kD and highly conserved sequences that are found in all eukaryotes [16]. Another tubulin, γ-tubulin, is not a part of the microtubules, yet it nucleates the polymerization of α- and β- subunits to form microtubules [1]. α- and β-tubulin are bound together by noncovalent bonds. Each α and β monomer has a binding site for GTP [5]. Each tubulin subunit has the ability to bind two molecules of GTP. GTP-binding site in α-tubulin binds GTP irreversibly and does not hydrolyze it to GDP. The nucleotide on the β-tubulin is exchangeable, because in β-tubulin GTP is bound reversibly and is hydrolyzed to GDP [17]. The nonexchangeable GTP is located between the α- and β-tubulin monomers, whereas the exchangeable GTP lies at the surface of the subunit [1]. The hydrolysis of GTP to GDP at this site has an important effect on microtubule dynamics [5]. The guanine

nucleotide which is bound to β-tubulin regulates the addition of tubulin subunits at the ends of the microtubule [3].

Microtubule is a hollow cylindirical structure of 24 nm in diameter that is built from 13 parallel protofilaments that are composed of α- and β- tubulin molecules [18]. Lateral and longitudinal interactions between the subunits are responsible for maintaining the tubular form. Longitudinal interactions link the subunits head to tail into a linear protofilament. The heterodimeric subunits repeat every 8 nm within each protofilament. By the lateral interactions, protofilaments associate side by side into a microtubule (Figure 1.3). A microtubule is a polar structure, and this polarity occurs because of the head-to-tail arrangement of the α- and β-tubulin dimers in a protofilament [1]. Subunits of each protofilaments in a microtubule point in the same direction. α subunits in a microtubule are exposed at the minus end while β subunits are exposed at the plus end [5].

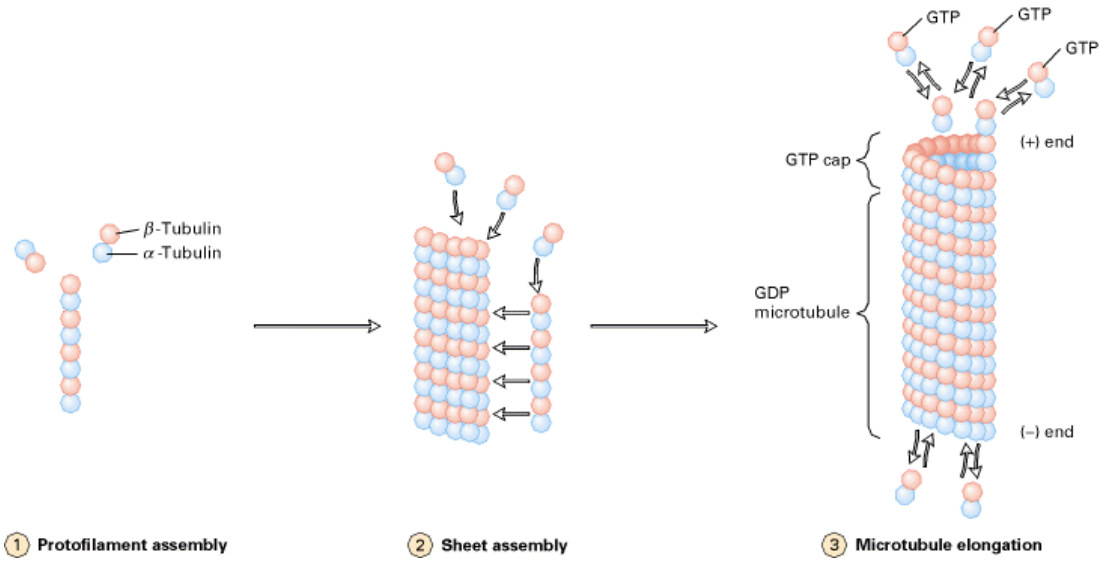

Figure 1.3. Assembly of microtubules. 1) Free tubulin dimers associate longitudinally to form protofilaments, 2) A sheet wraps around into a microtubule with 13 protofilaments, 3) Microtubule polymerization [1].

Microtubules form two types of structures: stable, long-lived microtubules and unstable, short-lived microtubules. Unstable microtubules assemble and disassemble quickly such as the cytosolic microtubule network in interphase cells during mitosis. In contrast to unstable microtubules, stable microtubules are usually found in non-

replicating cells such as the axoneme in the flagellum of sperm, the marginal band of microtubules in most red blood cells and platelets, and the axons of neurons [1, 18].

Microtubules assemble from a central organizing center by radiating in many interphase cells called microtubule-organizing center (MTOC) [19]. In animal cells, the MTOC is a centrosome. During mitosis, the centrosome duplicates and migrates to new positions. Duplicated centrosomes become the organization center for microtubules that form the bipolar mitotic apparatus. Then it will separate the chromosomes into the daughter cells during mitosis. In an interphase animal cell, the (-) ends of microtubules are proximal to the MTOC. In nerve cells, the (-) ends of axonal microtubules are oriented toward the base of the axon, but dendritic microtubules have mixed polarities [1, 20]. Some proteins are necessary for initiating the polymerization of microtubules. One of them is γ-tubulin. Introduction of antibodies against γ-tubulin into cells blocks microtubule polymerization process. That implicates γ-tubulin is necessary for nucleating assembly of tubulin subunits [1].

1.1.2.2. Microtubule Dynamics

A microtubule can undergo between growing and shortening phases, and this dynamic behavior lets the cell quickly assemble or disassemble microtubule structures. Microtubule assembly occurs by the polymerization of α- and β-tubulin dimers [15]. The polymerization process is temperature-dependent. If assembled microtubules are cooled down to 4 ºC, they depolymerize into dimeric subunits. And if tubulin dimers are warmed up to 37 ºC in the presence of GTP, they polymerize into microtubules [1]. Above the critical concentrations of tubulin dimers, microtubule polymerization initiates. Both assembly and disassembly occur faster at the (+) end than the (-) end [21]. Microtubule assembly occurs in three steps: tubulin dimers form protofilaments; protofilaments associate and form the wall of the microtubule; more subunits are added to the ends of protofilaments and the microtubule elongates [15].

As mentioned, above the C_c, tubulin subunits polymerize into microtubules, whereas below the C_c, microtubule depolymerization into tubulin subunits occurs. Under *in vitro* conditions, tubulin subunits add to one end and dissociate from the opposite end of the microtubule and this process is called “treadmilling”. In all cases, the rate of

microtubule lengthening is much slower than the rate of shortening. This property of microtubules is termed “dynamic instability” [1].

1.1.2.3. Microtubule-Associated Proteins (MAPs)

Microtubule-associated proteins (MAPs) have the ability to bind microtubules. They cross-link microtubules to one another and other structures in the cytosol [22]. Assembly MAPs are organized into two domains: a basic microtubule-binding domain and an acidic projection domain. The projection domain appears as a filamentous arm in the electron microscope and it extends from the wall of the microtubule. It can bind to membranes, intermediate filaments, other microtubules and its length controls how far apart microtubules are spaced [1, 23].

Assembly MAPs are grouped into two types by the sequence analysis. Type I MAPs are MAP1A and MAP1B. These are large and filamentous molecules and are found in axons and dendrites of neurons and also in non-neuronal cells [1].

Type II MAPs are MAP2, MAP4, and Tau (Figure 1.4). MAP2 is found only in dendrites. It forms fibrous cross-bridges between microtubules and also between microtubules and intermediate filaments. MAP4 is the most ubiquitous one and is found in neuronal and non-neuronal cells. MAP4 is thought to regulate microtubule stability during mitosis. Tau is found in both axons and dendrites and it is present in four or five forms derived from alternative splicing of a Tau mRNA. It cross-links microtubules into thick bundles and it may contribute to the stability of axonal microtubules [1, 22].

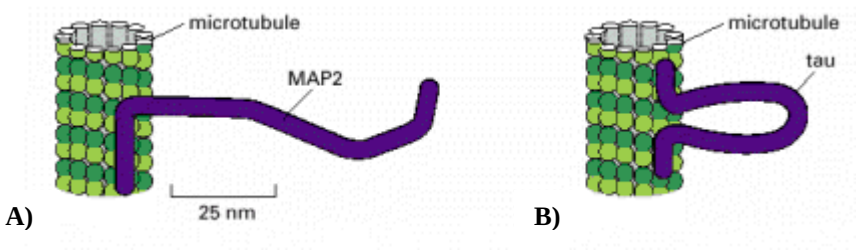

Figure 1.4. A) MAP2 binds along the microtubule lattice at one end and extends a long projecting arm with a second microtubule-binding domain at the other end. B) Tau binds to the microtubule lattice at both its N- and C-termini, with a short projecting loop [1].

Some MAPs like MAP4 and Tau stabilize microtubules but others do not. MAPs-coated microtubules are unable to disassemble. Hence, tubulin subunits can not dissociate when bound with MAPs. Some phosphorylating enzymes such as MAP

kinase (phosphorylating MAPs) and cdc2 kinase (phosphorylating MAP4) phosphorylate the projection domains of MAPs reversibly. Phosphorylated MAPs can not bind to microtubules and microtubule disassembly occurs [1, 23].

1.1.2.4. Intracellular Transport

Proteins, organelles and membrane-coated vesicles are transported to the defined addresses in the cytosol. Microtubules function as tracks in the intracellular transport of all these, and that movement is propelled by microtubule motor proteins [24] (Figure 1.5).

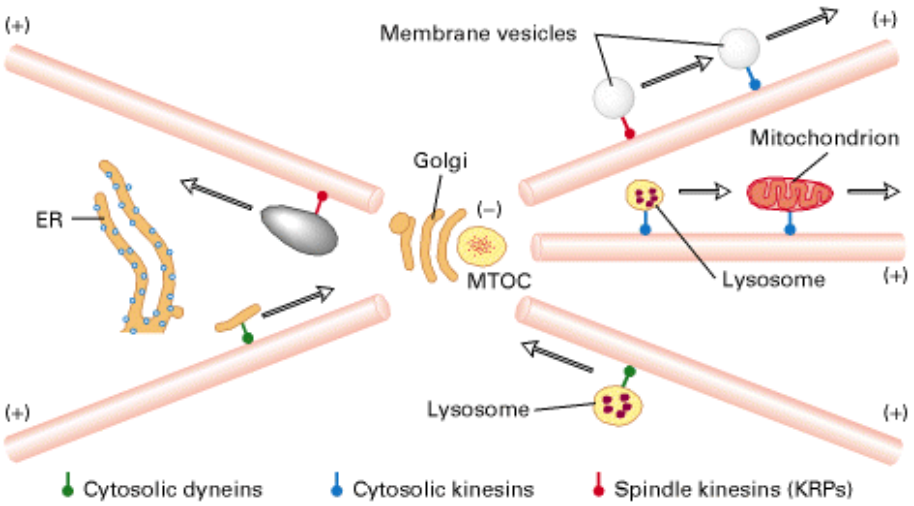

Figure 1.5. A general model for kinesin- and dynein-mediated transport in a typical cell. The array of microtubules, with their (+) ends pointing toward the cell periphery, radiates from a MTOC in the Golgi region [1].

Neuronal axons do not contain ribosomes, hence the protein synthesis only occurs in the cell body and dendrites of the neuron. Therefore, proteins synthesized in the cell body must be transported down to the axon. Axonal transport occurs on microtubules. In axons, microtubules are oriented with their (+) ends toward the terminal that is critical for axonal transport [25].

Melanophores, specialized pigment cells, are found in the skin of many amphibians and fish. Transport of the pigment granules throughout the cell or toward the center of the cell results in the change of the color of the skin. During these movements, microtubules serve as tracks along that the pigment granules can move in either direction [1, 24].

1.1.2.5. Kinesin and Dynein, Microtubule Motor Proteins

Kinesin

Kinesin is a dimer of two heavy chains and each is complexed with a light chain. It has a total molecular weight of 380,000. Kinesin has three domains, a pair of large globular head domains that is connected to a pair of small globular tail domains by a central stalk. Tail domains contain light chains. Each domain has a particular function. The head domain binds microtubules and ATP, and is responsible for the motor activity of kinesin. The tail domain binds membrane-bound vesicles that are referred to as kinesin's cargoes [1, 26].

Kinesin is a (+) end-directed microtubule motor protein. It walks towards the (+) end of the microtubule. Kinesin is responsible for anterograde and other (+) end-directed movements, such as the transport of secretory vesicles to the plasma membrane and the radial movements of endoplasmic reticulum membranes and pigment granules [24, 27].

Kinesin belongs to a family which has more than 12 different members. They all contain the kinesin motor domain, but their tail domains are different and they have different several other properties [1]. In most kinesins, the motor domain is at the N-terminus (N-type), but in some, the motor domain is central (M-type) or at the C-terminus (C-type). N- and M-type kinesins are (+) end-directed motors, whereas C-type kinesins are (-) end-directed motors. Also some kinesins are monomeric, whereas most are dimeric. These two types of kinesins differ in quaternary structure [28].

According to the cargo they transport, kinesins can be divided into two functional groups, cytosolic and spindle kinesins. Cytosolic kinesins are responsible for the transport of vesicles and organelles. Axonal kinesin is an example to them. It transports lysosomes and other membranous organelles. Some cytosolic kinesins are responsible for the transport of one specific cargo. For example, KIF1B transports mitochondria and KIF1A transports synaptic vesicles to the nerve terminal. Spindle kinesins function in spindle assembly and chromosome segregation during cell division. For example, the kinetochore-associated protein CENP-E, the spindle pole protein BimC, and a (-) end-directed motor called ncd [1, 25].

Dynein

Dynein is responsible for movement toward the (-) end of microtubules. Dyneins are large, multimeric proteins and their molecular weight exceeds 1,000,000 D. They have two or three heavy chains associated with intermediate and light chains [1].

Dyneins are divided into two groups according to their functions: cytosolic dyneins are involved in the movement of vesicles and chromosomes whereas axonemal dyneins are responsible for the beating of cilia and flagella. Cytosolic dynein has two head domains that are formed by two identical or nearly identical heavy chains [27].

Unlike kinesin, dynein can not mediate transport by itself. A large complex of microtubule-binding proteins are required for dynein-related motility. These proteins link vesicles and chromosomes to microtubules but do not exert force to cause movement. The best known complex is dynactin. It includes a protein called Glued, the actin-capping protein Arp1, and dynamatin [29]. In vitro experiments show that dynactin enhances dynein-dependent motility by the interaction with microtubules and vesicles. Glued has a microtubule-binding site at its N-terminal region. In this complex, the light chains of dynein interact with the dynamatin. As a model, dynactin tethers a vesicle to a microtubule, while dynein generates the force and polarity for movement [1, 29].

1.1.2.6. Microtubule Dynamics during Mitosis

During mitosis newly replicated chromosomes are separated into two daughter cells. The cell assembles and then disassembles a specialized microtubule structure called mitotic apparatus. The mitotic apparatus attaches and capture chromosomes, align and then separate them, so the genetic material is partitioned to each daughter cell [30]. This portion of the cell cycle is divided into four stages: prophase, metaphase, anaphase, and telophase. Mistakes in mitosis can lead to missing or extra chromosomes that result in developmental abnormalities during embryogenesis and pathologies after birth. Therefore microtubule motor proteins and microtubule dynamics have both crucial roles during mitosis [1, 30].

The mitotic apparatus has a changing structure during mitosis. Three distinct sets of microtubules form the mitotic spindle. Two centrosomes at the opposite poles organize the microtubules whose (-) ends all point toward the centrosome. First, the astral microtubules form the aster, they radiate outward from the centrosome to the

cell cortex. They help position the mitotoic apparatus and also have a role in determining the cleavage plane during cytokinesis. Second, kinetochore microtubules attach to chromosomes at particular sites on chromosomes called kinetochores. Third, polar microtubules do not interact with chromosomes, but they interdigitate with polar microtubules from the opposite pole. The mitotic spindle is composed of kinetochore and polar microtubules (Figure 1.6) [1, 30].

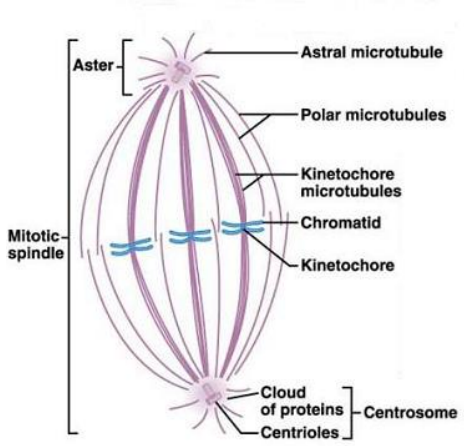

Figure 1.6. Three sets of microtubules in the mitotic apparatus [1].

First change in microtubule stability occurs at prophase during mitosis. Long interphase microtubules disappear and are replaced by a spindle and astral microtubules. The average lifetime of a microtubule decreases from 10 minutes in interphase cells to 30 seconds in the mitotic spindle. This high tubulin turnover enables microtubules to assemble and disassemble more quickly during mitosis [31].

Attachment of spindle microtubules to the poles and then capture of chromosomes by kinetochore microtubules are required for the assembly of the spindle. The two centrioles in the centrosome, the MTOC in most animal cells, are replicated during interphase. With the beginning of mitosis, they migrate to the two poles and organize the astral microtubules. Interactions between asters and the cell cortex and between opposing spindle microtubules separate and align the centrosomes during prophase. This establishes the bipolar orientation of the spindle. At metaphase spindle microtubules capture the kinetochores of chromosomes and center the chromosomes. Microtubule polymerization and depolymerization and microtubule motor proteins together holds chromosomes at the metaphase plate and translocates chromosomes to the opposite poles at anaphase. And during cytokinesis, cleavage occurs between the asters [1, 30, 32].

1.1.2.7. Some Drugs That Affect Microtubule Dynamics

Several drugs inhibit mitosis by affecting microtubule assembly and disassembly. Colchicine, taxol, and vinblastine are known to bind α- and β-tubulins or microtubules. Cochicine and colcemid have been used as mitotic inhibitors. With high concentrations of colcemid, cytosolic microtubules depolymerize and they leave MTOC, whereas at low concentrations, the microtubules remain and the cell becomes blocked at metaphase. When the cells are washed with a colcemid-free solution, colcemid diffuses from the cell and mitosis goes normally. If colchicine-bearing tubulins are added to the ends of a microtubule, addition or loss of other tubulin subunits are prevented. Taxol and vinblastine bind to microtubules and stabilize them. They inhibit microtubule dynamics, lengthening and shortening of microtubules.

Drugs which disturb the assembly and disassembly of microtubules have been widely used to treat various diseases. More than 2500 years ago, heart diseases had been treated with colchicine in the ancient Egypt. And now colchicine is used to treat gout and some other disease that affect the joints and skin. Taxol and vinblastine are effective anticancer agents, because blockage of spindle formation preferentially inhibits rapidly dividing cells like cancer cells. For example, taxol is used in the treatment of ovarian cancer cells. Taxol blocks mitosis in these cells but does not affect other functions performed by microtubules [1, 33].

1.2. XENOESTROGENS

Xenoestrogens are chemicals with diverse structures that mimic estrogen. These are pesticides and industrial by-products with little or no structural homology to estradiol that are common in the environment and act as agonists or antagonists of estrogens [34]. Because they mimic endogenous hormones or interfere with endocrine processes, they are called endocrine disrupters. Xenoestrogens are hydrophobic, and enter the body easily by diffusion through biological membranes, and accumulate in hydrophobic compartments of the cell, where they can disturb normal cellular functions. The proposed targets in cells include spindle microtubules, MT-associated proteins, kinetochores and centromeres, centrioles and centrosomes, as well as DNA. Two types of genetic changes can be thought; numerical chromosome changes (aneuploidy) with no apparent DNA damage, and structural chromosome aberrations

induced by catechol metabolites presumably through DNA damage. They may interfere with spindle apparatus during mitosis resulting abnormal segregation of chromosomes or inhibit MT assembly [35].

1.2.1. BISPHENOL A

Investigators from Stanford University identified an estrogen-binding protein in yeast and then investigated whether yeast have an endogenous ligand. After first reporting that yeast produce estradiol, they found that the estrogenic activity did not come from the yeast, but from culture media that were prepared with water autoclaved in polycarbonate flasks. With binding to estrogen receptor used as a bioassay, the estrogenic compound was purified and identified as bisphenol A (BPA) [34]. Bisphenol A is a common name for 2,2-(4,4-diydroxydiphenyl) propane [36].

The estrogenicity of bisphenols was reported for the first time in 1936 by Dodds and Lawson, who looked for synthetic estrogens devoid of the phenantrenic nucleus. Bisphenols were subsequently discarded for pharmaceutical purposes. In 1944, Reid and Wilson again studied the relationship of the structure of some bisphenols to estrogenic activity in vivo compared with stilbene derivatives. The early reported estrogenicity of bisphenols was not considered a toxicological problem, and new bisphenols were synthesized for use in many industrial applications. Concern about the estrogenicity of bisphenols in plastics and the consequences of human exposure to them was raised by Krishnan, who suggested that BPA was responsible for the estrogenicity of water sterilised in polycarbonate flasks. Rivas *et al*. later demonstrated the leaching of various bisphenols (BPA and methyl-BPA) from food cans and dental sealants (BPA and BPA dimethacrylate). Hashimoto and Nakamura showed the estrogenicity of a range of bisphenols used as dental materials [37].

It is thought that the estrogenic activity of these chemicals cause reproductive disorders and various types of cancer. The effects of these estrogens are thought to target the cytoskeletal structures such as microtubules. To show the effects of xenoestrogens on cytoskeletal proteins, we have chosen BPA.

1.2.1.1. Structure

Bisphenols is a broad term that includes many substances.They have two phenolic rings joined together through a bridging carbon as a common chemical structure

(Figure 1.7) [35, 37]. BPA is produced by an acid-catalyzed reaction of phenol and acetone and is composed of two unsaturated phenol rings [34].

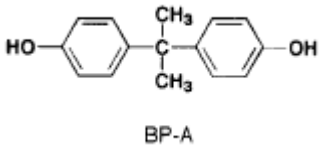

Figure 1.7. Chemical structure of bisphenol A [35].

Table 1 shows the physical and chemical properties of BPA.

Table 1.1. Physical and Chemical Properties of Bisphenol A [36].

Parameter	Value
CAS No.	80-05-7
Molecular Weight	228 g/mol
Formula	$C_{15}H_{16}O_2$
Specific Gravity	1.060 g/cm^3 1.195 g/cm^3
Boiling Point	220 °C (at 4 mmHg) 398 °C (at 760 mmHg)
Melting Point	150-155 °C 157 °C
PKa	9.59, 10.2 11.30
Water Solubility	120,000 μg/L 300,000 μg/L
Vapor Pressure	4.0E-8 mmHg 3.96E-7 mmHg 8.70E-10 mmHg 3.96E-9 mmHg

1.2.1.2. Usage

Bisphenols, in particular bisphenol A (BPA), are monomers of various plastics including polycarbonates, epoxy and other resins which are used in numerous consumer products [35]. Most BPA is used in the manufacture of polycarbonate (60%) and epoxy resins (30%), with the remaining 10% being used for the production of polyester resins. Polycarbonate, composed of BPA monomers, has many desirable commercial qualities such as transparency, moldability and high impact strength [34]. Polycarbonates are used in a variety of consumer products,

including a number of that come into contact with food, such as returnable beverage containers, infant feeding bottles, plastic dinnerware, and plastic storage containers. In addition, they are used in non-food consumer goods, such as eyeglass lenses, electrical equipment, household appliances, and sport safety equipment [38]. The carbonate linkages are rather stable, but can be hydrolyzed at high temperature and neutral pH, resulting in release of BPA. Epoxy resins are common lacquer-coatings of cans in the food industry and are also used for composites and sealants in dentistry [35]. Epoxy resins containing BPA diglycidylether (BADGE) have superior adhesive properties. When reacted with a hardener, they become cross-linked and can be used in coating or bonding applications. BPA diglycidyl methacrylate (bis-GMA) is a constituent of dental sealants used to replace tooth structures. Their polymerization (curing) reaction is photo-initiated by UV or visible light. Incompletely polymerized resins may contain 5-10% of free BPA [34]. BPA is also used in lesser amounts in various applications, for example, as an intermediary in thermal paper production and as an antioxidant and inhibitor of end polymerization in the manufacture of poly(vinyl chloride) plastics [38].

1.2.1.3. Exposure – Prevalence

Due to their use in food packing materials and many household products, bisphenols have the potential for widespread occupational and consumer exposure [35]. Because BPA is used in the manufacture of a variety of high-volume consumer products, there are a number of possible routes of exposure for members of the general population. These can be (1) direct and indirect environmental exposure due to the release of BPA during its production, use, and disposal; (2) exposure through leaching into food; and (3) contact with or inhalation of non-food-contact consumer products. BPA has been in use commercially for over 50 years, and workers producing this compound and its products (eg, epoxy resins) have been exposed to time-weighted average air levels to about 10 mg/m^3 over decades. From this experience, it has been found that high exposures to BPA are irritating to the eye and respiratory tract, and may cause skin lesions and photosensitization of the skin. No studies reporting systemic effects were identified, and no epidemiologic studies of workers who have been exposed occupationally were found [38].

For the last 40 years, substantial evidence has surfaced on the hormone-like effects of environmental chemicals such as pesticides and industrial chemicals in wildlife

and humans. The endocrine and reproductive effects of these chemicals are believed to be due to their ability to: (1) mimic the effect of endogenous hormones, (2) antagonize the effect of endogenous hormones, (3) disrupt the synthesis and metabolism of endogenous hormones, and (4) disrupt the synthesis and metabolism of hormone receptors. The discovery of hormone-like activity of these chemicals occured long after they were released into the environment [39]. Bisphenol A (BPA) is a particularly important environmental estrogen. Not only is it widespread in the environment, but it is commonly ingested by humans, being released by polycarbonate plastics, the lining of food cans, and dental sealants. BPA has a weak estrogenic activity *in vitro* and *in vivo*, but recent evidence indicates that this substance is able to interact with the estrogen receptor-α (ERa) in a unique manner, somewhat different from estradiol [40]. BPA has about 1/10000 the biological activity of estradiol [41].

These estrogenic compounds also alter cell cycle kinetics, induce DNA damages, and produce telomeric associations and chromosomal aberrations. Whether weak or strong, the estrogenic response of a chemical, if not overcome, will add extra estrogenic burden to the system, and particularly those endocrine disrupting environmental and industrial estrogen-like chemicals capable of producing genomic instability will induce additional burden of genomic instability. Though, estrogenically some of these compounds may be weak, they may have different activities in generation of genomic instability [42].

Biologic effects of BPA, which has been proven to interact with estrogen receptors, include enhancement of prolactin gene expression in pituitary cells, promotion of hyperplasia and differentiation in the female reproductive tract epithelium of rats, and acceleration of growth and puberty in female mice. In addition, estrogenic alkylphenols including BPA have been shown to induce apoptosis in several types of cells [43].

When given to pregnant mice, BPA crosses the placenta and reaches fetal organs. Cytochrome P_{450} works to reduce estrogens, and glucuronosyl-transferase degrades BPA. Since the fetus does not express this enzyme and BPA crosses the placenta, the fetus may lack protection from the effects of this exogenous estrogen [44]. Additionally, it binds to α-fetoprotein with affinity relative to estradiol, this results in

its enhanced bioavailability during neonatal development [45]. Also when given to mother during lactation, BPA is transferred to neonatal infants via milk [46].

Following the observation that BPA leached from autoclavable polycarbonate laboratory flasks, it was recently reported that BPA is released from the epoxy resin lining of food cans (4-23 μg per can; 7-380 μg/kg) and from restorative materials used in dentistry (90-913 μg in saliva collected in a 1-hour period following application of dental sealant) [35, 45]. Olea *et al*. have reported the presence of BPA in foods preserved by canning in polycarbonate-lined tin cans. It was found that BPA leaches from the treated teeth into saliva; up to 950 μg of BPA were retrieved from saliva collected during the first hour after polymerization [39].

There is increasing concern about the potential negative impact on public health of a class of environmental chemicals with estrogenic activity: the potential effects of these environmental estrogens include breast cancer, reduced sperms counts, and a variety of reproductive abnormalities [40]. Exposure to BPA with skin contact results in skin lesions and occupationally may result in photosensitisation in humans [47].

Additionally, results of some studies have shown that estrogenic chemicals including BPA and DES can act at very low doses in the range of human and wildlife environmental exposures [44].

BPA has been known to cause extensive damage to various organs in a human who absorbed it through the skin. It is also known to cause adverse reproductive effects in rats and mice [48].

BPA is able to affect in mice the development of reproductive organs and their function in the male offspring of mothers fed with this chemical during pregnancy [40]. Animal experiments indicated effects such as uterotrophic effects, decreasing sperm production, stimulation of prolactin release, promotion of cell proliferation in a breast cancer cell line and influence on preimplantation development [49].

Female rats treated with BPA by administration via drinking water during gestation produced male offspring with smaller testes. Low-dose exposure in mice has also been reported to result in increased prostate weight and reduced daily sperm production per gram testis [50].

Exposure of BPA within the range of human exposure (2-20 μg/kg) in pregnant mice during last gestation days resulted in small increases in prostate (30-36%) and preputial gland weights and small decreases in daily sperm production (20%) and epididymal weights (12%) of adult male offspring that are 6 months old [41].

Exposure of pregnant mice to 20 μg/kg BPA during last gestational days induced both vaginal opening and first vaginal estrus at a significantly earlier age in female offspring [45].

Exposure of the developing mouse fetus to BPA (25-250 μg/kg) showed that the virgin mice at puberty exhibit mammary glands that resemble those of pregnant mice. This is reflected by a significant increase in the percentage of ducts, terminal end buds, terminal ducts and alveolar buds [45].

BPA administration to female rats (100-1000 mg/kg) by gavage during the entire period of pregnancy produced pregnancy failure, pre- and postimplantation loss, fetal developmental delay and severe maternal toxicity [51]. To investigate the adverse effects of BPA on initiation and maintenance of pregnancy and embryofetal development, rats were administered to BPA during the entire period of pregnancy. The results indicated pregnancy failure, increased pre- and postimplantation loss, decreased fetal body weight and retarded fetal ossification at a maternally toxic dose. However, BPA did not induce embryofetal dysmorphogenesis [51].

It was shown that BPA induced cell proliferation and progesteron receptor synthesis in estrogen-dependent MCF-7 human breast cancer cells [52].

Iida *et al*. demonstrated that exposure of cultured Sertoli cells to BPA decreased the cell viability in a dose- and a time-dependent manner and that exposure to BPA brought about morphologic changes of the cells, such as membrane blebs, cell rounding, cytoskeletal collapse, and chromatin condensation or fragmentation, all of which conform to the morphologic criteria for apoptosis. Apoptosis-inducing cell death was observed in cells exposed to 150-200 μM BPA, while BPA at <100 μM had only slight cytotoxic effects on the cells [43].

Oral administration of BPA in mice and rats resulted in changes in size and nucleation of hepatocytes of liver in a 90-day study [47].

Oka *et al*. demonstrated that BPA induced marked malformations and specific apoptosis of central nervous system cells during early development of *Xenopus laevis* embryos, and that these BPA effects appeared to be due to non-estrogenic activities on developmental processes [53].

Suzuki *et al*. reported that, in goldfish at 8 days after treatment, BPA induced vitellogenin synthesis but decreased the plasma calcium level and inhibited secretion of the calcium-regulating hormone, calcitonin [54].

Katoh *et al*. concluded that BPA possessed a suppressing action on GH synthesis and release, and this suppressing action is probably related to impairment of cellular signal transduction systems in ovine anterior pituitary cells [55].

It was shown that BPA affected the transcriptional activities of thyroid hormone receptors in transfected human embryonic kidney cells [47].

During central nervous system (CNS) development, programmed neuronal cell death is an essential procedure in the early stages in which caspase-3 plays an important role. Because 17β-estradiol is known to have a protective effect against neuronal cell death against models of neurodegenerative disorders such as Alzheimer's disease, Negishi *et al*. hypothesized that BPA might influenced neuronal cell death and caspase-3 activation in cultured neurons. They showed the inhibitory effect of BPA on caspase-3 activity in CNS neurons and neuronal cell death in cultured neurons [56].

It is probable that endocrine disrupters also affect the differentiation and development of brains because the volume and/or the number of neurons in some hypothalamic nuclei are determined by the organizational action of estrogen, producing sex differences in the structure and function of the hypothalamic and extrahypothalamic nuclei [57].

Steinmetz *et al*. indicated that BPA induced molecular and morphologic alterations in the uterus and vagina of adult rats by inducing DNA synthesis and c-*fos* gene expression [44].

Neonatal treatment of rats with BPA and some other endocrine disrupting chemicals (EDCs) resulted in motor hyperactivity. It has been suggested that these EDCs might inhibit the development of dopamine neurons in brain. According to data, neonatal

treatment with EDCs provides an animal model of hyperkinetic disorder that includes the variation seen in a clinical setting [58].

Various aspects of non-social behavior are affected by perinatal exposure to BPA. This confirms the hypothesis that exposure to an environmental estrogen in the critical period of sexual differentiation can permanently influence the neural systems involved in the organization of behavior [40]. The effects of BPA on the sexual differentiation of the norepinephrine system and related behaviors were examined in rats. Pregnant rats were administered with BPA at a dosage that is less than the tolerable daily intake level during both pregnancy and lactation. The findings suggested that higher brain functions such as learning and emotional control are under the influence of chemical impacts including BPA [59].

Pregnant rats were exposed to BPA (40-400 μg/kg) from day 14 of gestation through postnatal day 6. Female offspring exhibited depressed motor activity and male offspring exhibited reduced anxiety-like behaviors [45]. Also, effects of BPA on maternal behavior were studied by giving low doses of BPA to adult female rats during pregnancy and lactation. BPA modified the behavior of mothers. Specific components of maternal behavior were reduced both active and passive, irrespective of the sex of pups and the period of observation [49].

Because estrogen and DES have been reported to induce immunosuppression and reduce host resistance to infectious disease, Konishi *et al*. examined the effects of BPA on immune system. BPA treated mice were injected with *E.coli* K-12. BPA pretreatment caused a decrease of T and B cell populations, macrophages and lymphocytes in the spleen of treated mice. When compared with non-treated mice, the eliminating activity in treated mice was diminished. Their results suggested that BPA possessed immunotoxicity and reduced the non-specific host defense as an acute toxicity [60]. Byun *et al*. also investigated the toxicity of BPA on immune responses. They proposed that BPA induced a generalized suppression of macrophage activation in vitro and nitric oxide (NO) and tumour necrosis factor (TNF)-α release are suppressed as well [61].

Takahashi *et al*. tested the mutagenicity of BPA using human RSa cells. The cells were treated with very low doses of BPA. They detected increased base substitution

mutations at K-*ras* codon 12 using PCR and dot-blot hybridization. This is the first study of base substitution mutations induced by BPA in human cells [62].

No epidemiological data relevant to the carcinogenicity of BPA are available. BPA was tested for carcinogenicity in 2-year feeding studies in rats and mice. In male and female rats, a small, not statistically significant increase in leukaemias was observed compared to the control group. Slight increases in the frequency of mammary gland fibroadenomas in male rats was thought to be a chance finding. In female rats, fibroadenoma incidence was not significantly increased. Also, an increased incidence in interstitial cell tumors (benign leydig cell tumors) in male rats was significantly higher both in the low-dose and the high-dose groups compared to the control group [63, 47]. In rats, body weight gain and feed consumption were reduced in treated groups compared to control groups. Other treatment-related findings were not observed [63].

Kabuto *et al*. suggested that pathological conditions caused by BPA may be related to the generation of reactive oxygen species and free radicals that are generated by BPA metabolism or estrogen-receptor-mediated systems. They also thought that BPA may affected reproductive and sexual characteristics by disturbing redox control systems. Their results showed that the injection of BPA induced overproduction of hydrogen peroxide in the mouse organs which is converted to hydroxy radical [64]. After that they investigated the modifications in endogenous antioxidant capacity and oxidative damage in the brain, liver, kidney and testis. Mice were exposed to BPA during embryonic, fetal life and lactation via their mothers. As a result, reactive oxygen species were induced in organs. Tissue oxidative stress and peroxidation were induced, ultimately leading to underdevelopment of the brain, kidney and testis [46].

In light of reports suggesting that low doses of BPA cause estrogenic effects in laboratory animals, concerns were raised about the safety of these consumer products, particularly plastic bottles used for feeding milk to babies. To evaluate the risk, if any, from BPA, investigations were undertaken to more precisely determine human exposure levels and more carefully study the validity of the low-dose effects reported. On the basis of the most realistic studies of BPA levels in food and drink, as well as in human urine, it has been estimated that human exposures, including those of children, are very low and range from about .001 to .1 mcg/kg body weight

(bw)/day. Human doses of BPA from migration of the compound into food and drink are orders of magnitude lower than acceptable daily intakes. Thus, it is very unlikely that humans, including infants and young children, are at risk from the presence of BPA in consumer products [38].

1.3. EFFECTS OF BPA ON MICROTUBULES

Several estrogens of diverse classes were studied for their ability to interfere with the assembly and disassembly of microtubules under cell-free conditions. Inhibition of microtubules in intact cells may lead to some changes such as the induction of micronuclei and aneuploidy. Thereby, they contribute to estrogen-mediated carcinogenesis. Natural estrogens, e.g., 17β-estradiol (E_2), and synthetic estrogens, e.g., diethylstilbestrol (DES) are known to be associated with human neoplasia. In experimental animals E_2 and DES as well as several of their analogs induce tumors in various tissues. In short-term assays, carcinogenic estrogens fail to induce gene mutations and DNA damage but lead to numerical and structural chromosomal aberrations. Several laboratories have reported that DES has colchicinelike effects, it causes the inhibition of microtubule polymerization under cell-free conditions as well as disruption of the mitotic spindle and the cytoplasmic microtubule complex in mammalian cells. The plastic estrogen bisphenol A (BPA) proved to be a powerful inhibitor that exhibits about half the activity of DES [65].

BPA disrupts the cytoplasmic microtubule complex and mitotic spindle (reversible) and can induce metaphase arrest and micronuclei in cultured Chinese hamster V79 cells. After treatment with BPA (200 μM), the mitotic spindle of all metaphase cells was no longer visible and diffuse tubulin stains were surrounded by chromosomes in an irregular arrangement. All these effects suggest that BPA and some of its analogs are potential aneuploidogens and microtubules are the main targets of DES and many other aneuploidogens [35, 66].

DES, E2 and BPA caused mitotic arrest and aberrant spindles, such as tripolar and multipolar spindles, in a concentration-dependent manner. Ochi *et al*. suggested that multiple microtubule nucleating sites were induced by the estrogens and BPA during the transition from interphase to the mitotic phase. DES, E2 and BPA induced multipolar division in a concentration-dependent process that is associated with the

induction of aneuploidy. The multipolar spindles are related to cell death, cell differentiation and malignant transformation via induction of an unequal chromosome distribution (aneuploidy). Also centrosome damage could be responsible for the induction of aberrant mitotic spindles. Centrosomes are composed of two centrioles that are surrounded by pericentriolar materials. Microtubules are nucleated on pericentriolar materials that are called microtubule-organizing centers (MTOCs). The MTOCs nucleate the microtubule assembly and form the microtubule polarity. So, centrosomal injury by estrogens could be involved in the induction of aberrant spindles. Ochi *et al*. demonstrated induction of multipolar spindles and alterations in centrosome organization as a mechanism for the induction of aberrant mitotic spindles by estrogens and BPA. Also it was demonstrated that induction of multipolar division by estrogens and BPA was associated with the induction of aneuploidy. The mitotic index of cells treated with BPA increased over the control levels [48, 67].

DES and its derivatives have been reported to inhibit microtubule assembly both in culture cells and in cultured cells. Also estradiol depolymerized the intracellular microtubule network in Chinese hamster V79 cells. It has been suggested that the induction of microtubule disruption is not related to binding of estrogens to their receptors. Nakagomi *et al*. suggested that some endocrine disrupting chemicals including DES, E2 and BPA have disruptive effects on the microtubule network in Chinese hamster V79 cells [66].

Hunt *et al*. encountered with a sudden, spontaneous increase in meiotic disturbances, including aneuploidy, in studies of oocytes from control female mice in their laboratory coincided with the accidental exposure of the animals to BPA. They identified that the damaged caging material and water bottles were the source of the exposure. In further experiments, they administered daily oral doses of BPA to directly test the hypothesis that low levels of BPA disrupt female meiosis. Finally, they demonstrated that the meiotic effects by BPA were dose dependent and could be induced by environmentally relevant doses of BPA. The exposure was correlated with highly significant increases in meiotic chromosome abnormalities, including nondisjunction and congression failure which is a specific meiotic phenotype at metaphase, therefore they implicated BPA as a potent disrupter of meiosis [68].

To investigate the aneuploidogenic potential of BPA, Lehmann *et al*. studied with cultured human AG01522C fibroblasts. In contrast to DES and 17β-estradiol, BPA did not induce micronuclei at any concentration. It inhibited the proliferation of the cultured cells in G2 phase and probably in G1 phase. Fluorescence microscopy of the BPA treated cells showed structural abnormalities of the cytoplasmic microtubule complex (CMTC) in a dose-dependent manner. The mitotic index did not increase and decrease in cell growth was dose-dependent. The mechanisms of growth inhibition and the interference with microtubules elicited by BPA in AG01522C cells are still unknown. Two mechanisms could be mentioned: (1) BPA may directly affect microtubules and impair their ability to depolymerize and repolymerize; and (2) BPA may primarily arrest the cell cycle and thereby affect microtubule dynamics [67].

Our project proposes to show the direct effects of BPA on microtubule proteins in vitro by sedimentation assay, fluorescence spectrometry and electron microscopy techniques. By using these techniques, we can analyze the possible changes in the assembly and disassembly properties of microtubules.

2. MATERIALS AND METHODS

2.1. Materials

2.1.1. Buffers for Tubulin Purification

2.1.1.1. 5X PM Buffer

500 mM Pipes-NaOH (Roche), 10 mM EGTA (Sigma) and 5 mM $MgSO_4.7H_2O$ (Riedel-de Haen) were dissolved in deionized water up to 1 lt. and pH was adjusted to 6.9 with NaOH. It was stored at 4°C.

2.1.1.2. 1X PM Buffer

5X PM buffer was diluted with deionized water five times and pH was adjusted to 6.9. It was stored at 4°C.

2.1.1.3. PM-4M Buffer

1X PM buffer containing 4 M glycerol (Carlo Erba) was prepared and stored at 4°C.

2.1.1.4. PM-8M Buffer

1XPM buffer containing 8 M glycerol (Carlo Erba) was prepared and stored at 4°C.

2.1.1.5. PMSF Solution

200 mM PMSF (Sigma) was dissolved in isopropanol (Merck) up to 10 ml and stored at room temperature.

2.1.2. Buffers for Ion-Exchange Column Purification

2.1.2.1. 1X PM

5X PM buffer was diluted with deionized water five times and pH was adjusted to 6.9.

2.1.2.2. 1X PM with GTP and DTT

0.1 mM GTP (Sigma) and 2 mM DTT (Sigma) were dissolved in 1X PM buffer up to 100 ml and pH was adjusted to 6.9.

2.1.2.3. NaOH Solution

0.5 M NaOH (Riedel-de Haen) was dissolved in deionized water up to 1.5 lt. and stored at 4°C.

2.1.2.4. HCl Solution

1.5 lt. 0.5 M HCl (37%) (Merck) was prepared and stored at 4°C.

2.1.3. Buffers for Experiments

2.1.3.1. AB Buffer

20 mM Pipes (Roche), 1 mM $MgCl_2$ (Riedel-de Haen) and 1 mM EGTA (Sigma) were dissolved in deionized water up to 1 lt. and pH was adjusted to 6.9 with NaOH. It was stored at 4°C.

2.1.4. Solutions for SDS-PAGE (Sodium Dodecyl Sulfate – Polyacrylamide Gel Electrophoresis)

2.1.4.1. Acrylamide Monomer Solution (30% T/ 2.7% C_{bis})

58.4 g Acrylamide (Sigma) and 1.6 g Bis-acrylamide (Sigma) were dissolved in deionized water up to 200 ml and stored in dark at 4°C.

2.1.4.2. 4X Running (Separating) Gel Buffer

36.3 g Tris (Meck) was dissolved in deionized water up to 200 ml and pH was adjusted to 8.8 with HCl. It was stored at 4°C.

2.1.4.3. 4X Stacking Gel Buffer

3 g Tris (merck) was dissolved in deionized water up to 50 ml and pH was adjusted to 6.8 and stored at 4°C.

2.1.4.4. 10% SDS

10 g SDS (99%) (Sigma) was dissolved in deionized water up to 100 ml and stored at room temperature.

2.1.4.5. 10% Ammonium Persulfate (APS)

0.1 g APS (Sigma) was dissolved in deionized water up to 1 ml and stored at 4°C. APS has a two week life.

2.1.4.6. TEMED (N, N, N', N' – Tetramethylethylene diamine)

TEMED (Farmitalia Carlo Erba S.p.A.) was used as purchased.

2.1.4.7. 2X Sample Buffer

2.5 ml 4X Stacking Gel Buffer, 4 ml 10% SDS solution, 2 ml Glycerol (20% glycerol) (Carlo Erba), 1 ml β- mercaptoethanol (Merck) and 0.05% Bromophenol Blue (BRB) (Sigma) were mixed with deionized water up to 10 ml. It was stored at -20°C as aliquots of 1.5 ml.

2.1.4.8. Tank Buffer (Running Buffer)

3 g/L Tris (Merck), 14.4 g/L Glycine (Merck) and 1 g/L SDS were dissolved in deionized water up to 1 lt. and stored at 4°C.

2.1.4.9. Coomassie Blue Stain

0.1% CBB R-250 (Fluka) was dissolved in 1 lt. deionized water containing 50% Methanol (Merck) and 10% Acetic acid (Merck). It was stored at room temperature.

2.1.4.10. Gel Destain

50 ml (1:20) Methanol and 100 ml (1:10) Acetic acid were mixed with deionized water up to 1 lt. It was stored at room temperature.

2.1.5. Stock Solutions

2.1.5.1. GTP Stock

200 mM GTP (Sigma) was dissolved directly in deionized water and stored at -20°C as aliquots of 20 μl.

2.1.5.2. DTT Stock

1 M DTT (Sigma) was dissolved directly in deionized water and stored at -20°C as aliquots of 1 ml.

2.1.5.3. Taxol Stock

10 mM Taxol (Paclitaxel, Sigma) was dissolved in DMSO (dimethyl sulfoxide) (Riedel-de Haen) and stored at -20°C.

2.1.5.4. Bisphenol A Stock

Bisphenol A (BPA) (Sigma) (10 mM) was dissolved in DMSO (Riedel-de Haen) and stored at 4°C.

2.1.6. Cellulose Phosphate Resin

Cellulose Phosphate Cation Exchanger (Whatman) was used for ion-exchange column preparation.

2.1.7. Solutions for Determination of Protein Concentration

2.1.7.1. Bradford Reagent

Bradford Reagent (Sigma) was used as purchased.

2.1.7.2. Bovine Serum Albumine (BSA)

14.5 mg/ml BSA (Sigma) was dissolved in deionized water up to 10 ml and stock standard solutions were prepared from that. They were stored at -20°C.

2.1.8. Solutions for Electron Microscopy

2.1.8.1. Pioloform

250 mg Pioloform (Agar Scientific) was dissolved in 100 ml chloroform (Merck). It was waited at 4° C for 10 days before use and kept in dark place.

2.1.8.2. Gluteraldehyde

40 µl Gluteraldehyde (Merck) was mixed with deionized water to make 4% (v/v) and stored at room temperature.

2.1.8.3. Uranyl Acetate

Uranyl Acetate (Sigma) was dissolved in deionized water to make 2% (w/v) and stored at room temperature.

2.1.9 Protein Marker

Benchmark Prestained Protein Ladder (Gibco) was used as a standard to analyze the SDS-PAGE gels. It consists of 10 proteins ranging in molecular weights of 10, 15, 20, 30, 40, 60, 70, 90, 130, and 220 kDa.

2.1.10 Lab Equipment

Autoclaves	: 2540 ML Benchtop Autoclave, Systec GmbH Labor-Systemtechnik.
	: NuveOT 4060 vertical steam sterilizer, Nuve.
Balances	: Precisa BJ 610C, order# 160-9423-050, Precisa Instruments AG, Dietikon.
	: Precisa XB 220A, order# 320-9204-001, Precisa Instruments AG, Dietikon.
Centrifuges	: Avanti J-30I, Beckman Coulter.
	: Optima LE80K, Beckman Coulter.
	: Optima Max, Beckman Coulter.
	: Allegra 25R, Beckman Coulter.
Centrifuge rotors	: JLA-16250, Beckman Coulter.
	: 70Ti, Beckman Coulter.
	: MLA 80, Beckman Coulter.
	: TS-5.1-500, Beckman Coulter.
Deep freezers and refrigerators	: 2031 D Deep Freezer, Arcelik.
	7751 T, Beko.
Electron Microscope	: JEM 1011 Transmission Electron Microscope, Joel.
Electrophoresis equipments	: EC 120 Mini Vertical Gel System, ThermoEC.

Fluorescence Spectrometer	: LS-50, Perkin Elmer.
Fraction Collector	: Model 2110, Bio-Rad.
Gel documentation system	: UVIpro GAS7000, UVItec Limited.
Gel dryer	: Model 583, Bio-Rad.
Glassware	: Technische Glaswerke Ilmenau GmbH.
Grids	: 300 mesh size copper grids, Sigma.
Homogenizator	: Potter S, B.Braun Biotech International
Ice machine	: AF 10, Scotsman.
Incubators	: EN400, Nuve.
Laminar Flow Cabinet	: Ozge.
Magnetic stirrer	: AGE 10.0164, VELP Scientifica srl.
	: AGE 10.0162, VELP Scientifica srl.
Microwave	: MD582, Arcelik.
Peristaltic pump	: Bio-Rad.
pH meters	: MP 220, Mettler Toledo International Inc.
	: Inolab pH level 1, order# 1A10-1113, Wissenschaftlich-Technische Werkstätten GmbH & Co KG.
Pipettes	: 0.1-2.5, 500-5000, Mettler Toledo.
	: 10, 20, 200, 1000, Gilson.
Pipette tips	: 1-1000 µl, 1-200 µl Axygen.
	: 1-10 µl, Molecular Bioproducts.
	: Gel loading tip, 10 µl, Molecular Bioproducts.
Power supply	: EC 250-90, E-C Apparatus.
Pure water systems	: USF Elga UHQ-PS-MK3, Elga Labwater.
Shaker	: Duomax 1030, Heidolph Instruments.

Spectrophotometers	:DU530 Life Science UV/Vis, Beckman.
	: UV-1601,Shimadzu Corporation.
	: Lambda 25 UV/Vis, Perkin Elmer.
Test tubes	: 1.5 ml tubes, Eppendorph.
Vacuum pump	: 262 BR, Bio-Rad.
Vortexing machine	: Reax Top, Heidolph Instruments.
Water bath	: Memmert.

2.2. Methods

2.2.1. Tubulin Purification

- One bovine brain was used for tubulin purification.
- Cerebellum and meninges with blood vessels were removed. And the remaining brain was weighed.
- The brain was minced with scissors.
- For each 100 g of brain, 75 ml PM-4M buffer containing 1 mM PMSF and 1 mM DTT was added into a blender and mixed.
- The homogenate was centrifuged with Beckman Avanti J-30I centrifuge, JLA-16250 rotor, 250 ml tubes at 30,000 x g and 4°C for 30 minutes.
- Supernatants were collected and centrifuged with Beckman Optima LE80K centrifuge, 70Ti rotor, 35 ml tubes, at 183,960 x g and 4°C for 40 minutes.
- Supernatants were collected and the total volume was named as V_1.
- 200 mM GTP was added and resulting mixture was incubated at 37° C for 30 minutes.
- The mixture was centrifuged with Beckman Optima LE80K centrifuge, 70Ti rotor, 26.3 ml tubes, at 183,960 x g (and Beckman Optima Max Ultracentrifuge, MLA 80 rotor, 10 ml tubes, at 184,262 x g) at 37° C for 30 minutes.
- Supernatants were decanded and pellets were taken onto ice and resuspended with $0.25xV_1$ ml of 1xPM buffer containing 1 mM PMSF and 1 mM DTT.
- The resuspended solution was homogenized with Potter S Homogenizator on ice and incubated at 4° C for 30 minutes.
- The homogenate was centrifuged with Beckman Optima Max Ultracentrifuge, MLA 80 rotor, 10 ml tubes, at 184,262 x g and 4° C for 30 minutes.
- The supernatants were collected and named as V_2.
- Equal volume (V_2) of PM-8M buffer was added; total volume= $2xV_2$.
- 1 mM PMSF, 1 mM DDT and 2 mM GTP were added into total volume.

- Mixture was incubated at 37° C for 30 minutes.
- Mixture was centrifuged with Beckman Optima Max Ultracentrifuge, MLA 80 rotor, 10 ml tubes, at 184,262 x g and 37° C for 30 minutes.
- Supernatants were decanded and pellets were resuspended with 0.25x V_2 ml of PM buffer.
- The resuspended solution was homogenized with Potter S Homogenizator on ice and incubated at 4° C for 30 minutes.
- The homogenate was centrifuged with Beckman Optima Max Ultracentrifuge, MLA 80 rotor, 10 ml tubes, at 184,262 x g and 4° C for 30 minutes.
- Supernatants were collected, named as semipurified tubulin and kept at -80° C as aliquots.
- The concentration of tubulin protein was determined by Bradford Assay.

2.2.2. Bradford Assay

- 14.5 mg Bovine Serum Albumin (BSA) was dissolved in 10 ml deionized water.
- Stock standard solutions were prepared as containing concentrations of 20 µg/ml, 40 µg/ml, 60 µg/ml, 80 µg/ml, 100 µg/ml, 120 µg/ml, 140 µg/ml, 160 µg/ml, 180 µg/ml, 200 µg/ml, 220 µg/ml, 240 µg/ml, 260 µg/ml, 280 µg/ml and 300 µg/ml BSA.
- From each stock standard solution, 100 µl was added to tubes for standard preparation.
- Then 900 µl Bradford reagent was added to each tube (total 1 ml).
- Sample preparation: sample amount was completed with deionized water up to 100 µl.
- Then 900 µl Bradford reagent was added to each tube (total 1 ml).
- Blank solution was prepared to zero spectrophotometer: 100 µl deionized water with 900 µl Bradford reagent.
- Both standard solutions and samples were transferred into spectrophotometer cuvettes just before measurement.
- The absorbance values and protein concentrations were measured at 595 nm with Beckman DU530 UV/Vis Spectrophotometer.

2.2.3. Further Tubulin Purification

2.2.3.1. Cellulose Phosphate Ion-Exchanger Column Preparation

- The volume of glass column was measured and named as V.
- V/4 g of phosphocellulose resin was weighed and put into a beaker.
- 25xV/4 ml 0.5 M NaOH was added and stirred gently, and left for 5 minutes.
- The supernatant was decanded and washed with deionized water until the filtrate pH was 11.0 or below.
- Then 25xV/4 ml 0.5 M HCl was added and stirred kindly, and left for 5 minutes.
- The supernatant was decanded and washed with deionized water until the filtrate pH was 3.0 or above.
- The supernatant was decanded completely and 25xV/4 ml 1x PM buffer was added.
- The pH was adjusted to 6.9 with NaOH.
- The resin was poured into the column.
- When all slurry was added, the cap of the column was attached.
- 1x PM buffer was run through the column until the column bed height was constant.
- 150 ml 1x PM buffer containing 0.1 mM GTP and 2 mM DDT was run through the column.
- The pH of the eluate was checked to be 6.9.
- The column was left overnight at 4° C.
- All these steps were completed at 4° C.

2.2.3.2. Further Tubulin Purification

- The fraction collector was attached with Bio-Rad peristaltic pump connected to the outlet of the column.
- Certain amount of semipurified tubulin solution was loaded to the column.
- Approximately V/2 ml of 1x PM buffer was run through the column with the flow rate of 2.5 ml/min.
- 1 to 12 fractions were collected as 2.5 ml and rest of the fractions were collected as 0.6 ml.

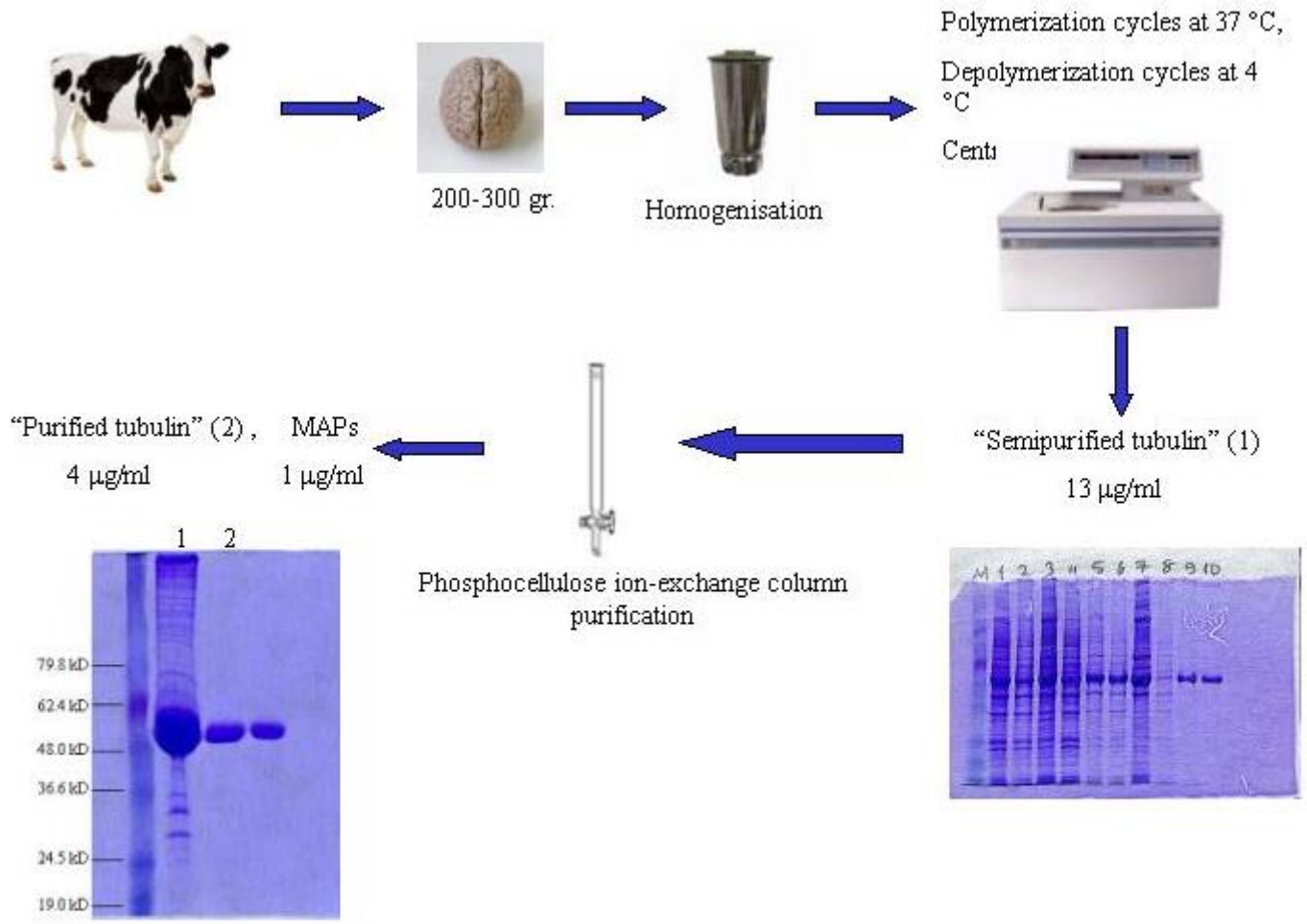

Figure 2.1. Scheme of tubulin purification.

- 10 µl samples were taken from each fraction and analyzed by Bradford reagent to determine which fractions contained protein.
- The fractions containing protein were pooled and the concentration was measured by Bradford Assay.

2.2.3.3. Elution of Microtubule-associated proteins from the column

- After tubulin proteins were obtained, microtubule-associated proteins were eluted from the column.
- 200 ml 1X PM buffer containing 1 M NaCl was run through the column and the fractions were collected.
- 10 µl samples were taken from each fraction and analyzed by Bradford reagent to determine which fractions contained protein.
- To determine the MAP fractions 7% SDS-PAGE gel was run and the fractions containing protein were pooled.
- Then MAPs were centrifuged with Beckman Allegra 25R, TS-5.1-500 rotor, Amicon-Centriplus centrifugal filter devices at 1396 x g, at 4°C for several hours.
- The filtered buffer was decanded and centrifugation was continued until MAPs were concentrated to 1/5 of its starting volume.
- MAPs were washed three times with 1X PM buffer to decant from salt.
- Then MAPs were collected by centrifugation.
- The concentration of MAPs was measured by Bradford Assay.

2.2.4. Sedimentation Assay

- Microtubule sedimentation assays were performed in AB buffer.
- Tubulin proteins from -80° C were thawed on ice.
- In a reaction volume of 100 µL, tubulin (5 µM final) or taxol-stabilized MTs (TMTs) were incubated with or without GTP (1 mM) in the presence of bisphenol A (BPA) with various concentrations (10, 50, 100, 200 µM).
- Preparation of TMTs: tubulin (10 µM) was incubated with GTP (1 mM) and taxol (100 µM) at 37° C for 30 minutes.
- BPA was dissolved in dimethyl sulfoxide.

- Control reactions contained no BPA.
- Additional control reactions with DMSO (final concentration 0.05%) were performed.
- After incubation for 30 minutes at 37° C, reactions were centrifuged at 127,960 x g for 30 minutes at 37° C with Beckman Optima Max Ultracentrifuge.
- The supernatants were transferred into tubes containing equal amounts of 2x SDS sample buffer, and the pellets were resuspended in 100 µL of 1x SDS sample buffer.
- Supernatant and pellet fractions were then analyzed by SDS-PAGE.
- For quantitative analysis, the amount of supernatant and pellet samples loaded onto the gels was optimized to ensure a linear relationship between the amount of protein loaded and the intensity of the Coomassie blue stained protein bands.
- The amount of MT proteins in the supernatant and the pellet fractions was quantified by mesuring the protein band intensities relative to standards with UVIpro GAS7000 Gel Documentation and Analysis System, Quantification Analysis UVITech UVIBand Map V99.01 Software.

2.2.5. SDS-PAGE

- Supernatants and pellets were separated.
- For each 100 µl of supernatant, 100 µl 2x sample buffer was added and mixed with vortex.
- For each pellet, 100 µl 1x sample buffer was added and mixed with vortex.
- 5 µl samples from pellet solutions and 10 µl samples from supernatant solutions were loaded onto SDS-PAGE gels using micropipette and loading tips.

2.2.5.1. Assembly of Gel

- Glass plates and spacers were cleaned with ethanol.
- They were assembled in gel holder on casting stand.
- Upper and lower screws were tightened and bottom edges of gel plates were checked.

- Smaller plate was marked 1.5 cm from top.

2.2.5.2. %10 Running (Separating) Gel Preparation

- 1.67 ml %30 acrylamide, 1.25 ml 4x running gel buffer, 1.97 ml deionized water, 50 µl %10 SDS, 30 µl %10 APS and 10 µl TEMED were mixed and poured between the glass plates up to the mark.
- When the gel was polymerized, the top of the gel was rinsed with tank buffer.
- Remaining water was absorbed with filter paper.

2.2.5.3. %4 Stacking Gel Preparation

- 0.27 ml %30 acrylamide, 0.5 ml 4x stacking gel buffer, 1.9 ml deionized water, 20 µl %10 SDS, 10 µl %10 APS and 5 µl TEMED were mixed and poured onto the running gel to the top of the front plate.
- A comb was placed into the stacking gel quickly.
- Gel was left for polymerization.
- After polymerization the comb was removed carefully.
- Lanes were washed with tank buffer and dried with filter paper.
- 5 µl samples from pellet solutions and 10 µl samples from supernatant solutions were loaded onto SDS-PAGE gels using micropipette and loading tips.
- Gel was run at 200 mV for approximately 45 minutes with E-C Apparatus Corporation, EC 250-90 power supply.
- Then the glass plates were separated and the gel was placed in Coomassie Blue stain in a clean box.
- The gel was microwaved at 750 Watt for 40 seconds.
- Then the gel was placed on shaker for 2 minutes.
- The stain was poured off and the gel was rinsed with gel destain.
- The gel was covered with gel destain and microwaved at 750 Watt for 50 seconds.
- It was placed on shaker for 15 minutes.
- Then destain was poured off and replaced with fresh destain solution.
- It was left overnight on shaker.
- The gel was dried with Bio Rad Model 583 Gel Dryer for storage.

- After scanning of dry gel, it was analysed with UVIpro GAS7000 Gel Documentation and Analysis System, Quantification Analysis UVITech UVIBand Map V99.01 Software.

2.2.6. Fluorescence Spectrometry

- Spectrometric mesurements were performed in AB buffer using the Model LS-50 spectrometer of Perkin-Elmer, equipped with a temperature controller.
- In a reaction volume of 3 ml, tubulin (10 μM) protein was mixed with BPA (200 μM) and GTP (1mM).
- Samples were excited at 295 nm and variation in the fluorescence spectra and emission intensity of the tryptophan residues in tubulin were monitored at 336 nm as a function of polymerization time during 1 hour incubation at 37°C.
- Control reactions were performed without BPA.

2.2.7. Electron Microscopy

2.2.7.1. Reaction Conditions

Control 1: 10 μM semi-purified tubulin + 5 mM GTP + 100 μM Taxol
Control 2: 10 μM semi-purified tubulin + 5 mM GTP
Reaction 1: 10 μM semi-purified tubulin + 5 mM GTP + 100 μM Taxol + 100 μM BPA
Reaction 2 : 10 μM semi-purified tubulin + 5 mM GTP + 100 μM BPA

2.2.7.2. Coating Grids with Pioloform

- Grids were put into 100% ethanol then chloroform before use then left for drying.
- Pioloform (250 mg) was dissolved in chloroform (100 ml). It was waited at 4° C for 10 days before use and kept in dark place.
- A glass block was plunged into pioloform solution and pulled out. Then it was left for drying in upright position approximately 2 min.
- The edges of the film on glass block were cut with a razor.
- The glass block was plunged into clean water and the film was left on water.
- Grids were put on the swimming film as their bright sides on the top.

- A clean slide was come near to the film and covered on it. Therefore, film covered grids were adhered to the slide.
- The slide was put into a clean dish and waited at 37° C for 1 day.

2.2.7.3. Preparation of Electron Microscopy Grids

- Polymerization of microtubules were carried out with freshly thawed microtubule proteins.
- All reactions were completed with AB buffer up to 100 µl in 1.5 ml test tubes.
- The tubes were incubated at 37° C in water bath for 1 hour.
- They were centrifuged with Beckman Optima Max Ultracentrifuge, MLA-80 rotor, at 127,960 x g, 37° C for 30 minutes.
- The supernatants were decanded.
- 20 µl 4% gluteraldehyde was added onto pellets and left for 15 minutes for fixation.
- Pellets were resuspended with micropipette one or two times gently.
- Grids were plunged into tubes and waited for 20 seconds.
- Then grids were washed by plunging into distilled water three times.
- Grids were left for air-dry for 30 minutes and stained.

2.2.7.4. Staining

- One drop of 2% uranyl acetate for each grid was put onto parafilm.
- Grids were placed on drops upside down and left for 2 minutes.
- Grids were washed by plunging into distilled water two times.
- Excess water was removed with filter paper.
- Grids were left for air-dry.
- Grids were analyzed with Joel Jem 1011 Transmission Electron Microscope.

3. RESULTS AND DISCUSSION

The aim of this study is to investigate the effects of BPA, an environmental estrogen, on cytoskeletal proteins, primarily on microtubules. For this reason, microtubules were purified from bovine brain with two cycles of polymerization and depolymerization method. Then, a further purification was performed with the phospho-cellulose ion-exchange column to obtain pure tubulin protein without microtubule-associated proteins (MAPs).

To analyze the effects of BPA on microtubule assembly and disassembly dynamics, we have employed sedimentation assays, fluorescence spectroscopy and electron microscopy experiments.

3.1. Tubulin Purification

A fresh bovine brain from butchery was taken to the laboratory immediately on ice. The cerebellum and meninges with blood vessels were removed. The remaining parts were weighed and the tubulin purification procedure was performed according to two cycles of polymerization and depolymerization method as mentioned before. At the end of this preparation, tubulin proteins were obtained together with microtubule associated proteins (MAPs) and called ‘semi-purified tubulin’. Then, the protein concentration was determined by the Bradford protein assay using bovine serum albumin (BSA) as a standard. To observe the purification steps, samples from each fraction of the procedure were run on an SDS-polyacrylamide gel (Figure 3.1).

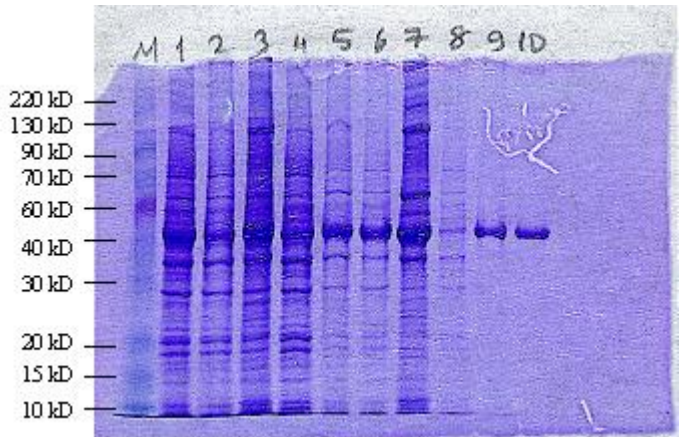

Figure 3.1. Tubulin purification fractions after two cycle of polymerization and depolymerization procedure. M, protein marker; 1, first depolymerization supernatant; 2, first polymerization supernatant; 3, first polymerization pellet; 4, second depolymerization supernatant; 5, second depolymerization pellet; 6, second polymerization supernatant; 7, second polymerization pellet; 8, third depolymerization supernatant; 9, third depolymerization pellet; 10, tubulin.

MAPs bind to polymerized microtubules or unpolymerized tubulins. This binding speeds up polymerization, facilitates assembly and stabilizes microtubules. To separate tubulin proteins from MAPs, phospho-cellulose ion-exchange column was prepared. Ion-exchange column purification separates molecules based on differences between the charge of the proteins. The phospho-cellulose column used in this purification was a cation column. In a cation exchange separation, positively charged proteins bind to the stationary phase in the column. Since MAPs are positively charged, they remained in the column attached to the resin and negatively charged tubulin proteins passed through the column.

Certain amount of semi-purified tubulin was loaded to the column and then PM buffer was run through. All the fractions collected were qualitatively analyzed with Bradford reagent for the presence of tubulin protein. Bradford reagent contains Coomassie Brilliant Blue G-250 dye which binds to proteins. This binding of CBB G-250 causes a color change indicating the presence of the protein. The fractions which contained color change were pooled into a tube. First, an SDS-PAGE (10%) was run to ensure whether or not fractions include any MAPs. After the column purification, one tubulin fraction could be seen free of MAPs. Also pure tubulin (99%) purchased from Cytoskeleton was run on the gel as a standard (Figure 3.2).

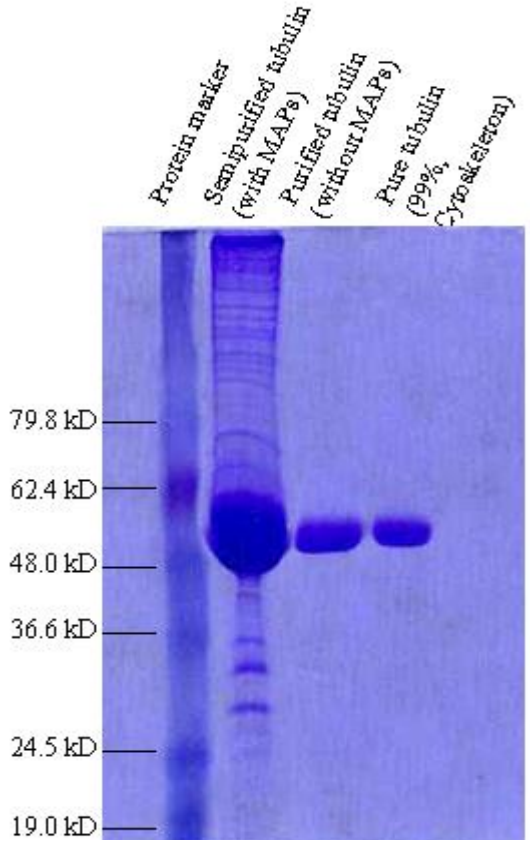

Figure 3.2. Semi-purified tubulin and purified tubulin after column purification. Each tubulin monomer (α/β) has a molecular weight of 55 kDa. The first fraction containig semi-purified tubulin with MAPs fractions can be seen. The second fraction is purified tubulin that was obtained after column purification (free of MAPs). The third fraction belongs to pure tubulin (99%) which was purchased from Cytoskeleton.

3.1.1. Elution of MAPs from phospho-cellulose column

While negatively charged tubulin proteins passed through the phospho-cellulose column, positively charged MAPs were bound to the resin. To elute MAPs from the column, PM buffer containing 1 M NaCl was run through. The eluted buffer which contained MAPs was collected as fractions. Small amounts of Bradford reagent was added into samples from these fractions to detect the presence of proteins. Then, samples from some fractions that contain protein were run on an SDS-polyacrylamide gel (Figure 3.3).

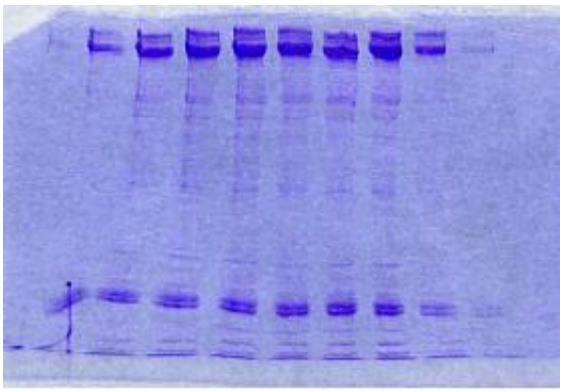

Figure 3.3. SDS-PAGE gel showing several MAP fractions.

Then MAPs were concentrated about five fold with Amicon-Centriplus centrifugal filter devices using Beckman Allegra 25R centrifuge. The concentration of MAPs were determined by Bradford assay using BSA as a standard.

3.2. Sedimentation Assays

To analyze the effects of BPA on microtubule polymerization, we have employed a microtubule sedimentation assay. Tubulin proteins from -80° C were first thawed on ice. In this assay, either semi-purified (spTb) or purified tubulin (pTb) proteins were used. In a reaction volume of 100 µl, tubulin proteins (final concentration 5 µM) and BPA (200 µM) were mixed in AB buffer (20 mM Pipes, 1 mM $MgCl_2$ and 1 mM EGTA). GTP (1 mM) was added to the reactions of pTb. Control experiments were performed without BPA. Since BPA was dissolved in dimethyl sulfoxide (DMSO), additional control reaction mix with DMSO were also performed. The final proportion of DMSO in the reactions was 0.05%. After reactions were set, the tubes were incubated at 37° C for 30 minutes. Then, they were centrifuged at 127,960 x g (50,000 rpm), at 37° C for 30 minutes with Beckman Optima Max Ultracentrifuge. The principle of the sedimentation assay is based on the microtubule polymerization. When microtubules are centrifuged above 100,000 x g, polymerized microtubules precipitate in the pellet and unpolymerized tubulin subunits remain in the supernantant. After centrifugation, supernatants and pellets were separated and supernatants were transferred into other tubes containing equal amounts of 2x SDS sample buffer. Pellets were resuspended with 100 µl of 1x SDS sample buffer. Both fractions were run on 10% SDS-PAGE. For quantitative analysis, the amount of supernatant and pellet samples loaded onto the gels were optimized to ensure a linear

relationship between the amount of protein loaded and the intensity of the Coomassie blue stained protein bands. The amount of microtubule proteins in the supernatant and in the pellet fractions were quantified by measuring the protein band intensities relative to standards with UVIpro GAS7000 Gel Documentation and Analysis System, Quantification Analysis UVITech UVIBand Map V99.01 Software. To compare the amount of protein in all fractions, we prepared protein standards which contained 1, 3, and 5 μM tubulin.

Sedimentation experiments with spTb were performed with various concentrations of BPA (10, 50, 100, 200 μM) to get the dose-response results and the effective BPA concentration. The densities of the pellet fractions in BPA-treated reactions were lower than the density of pellet fraction in control reaction. The SDS-PAGE results indicated that formation of microtubules from spTb was inhibited at 37°C in the presence of BPA (Figure 3.4).

The inhibition of microtubule polymerization caused by BPA was observed in a dose-dependent manner (Figure 3.5).

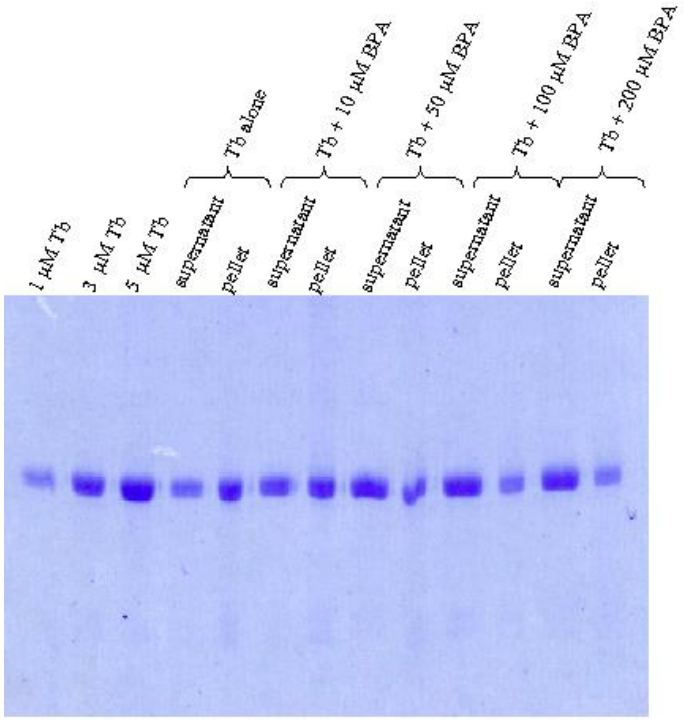

Figure 3.4. Effects of various doses of BPA on microtubule polymerization on the same SDS-polyacrylamide gel.

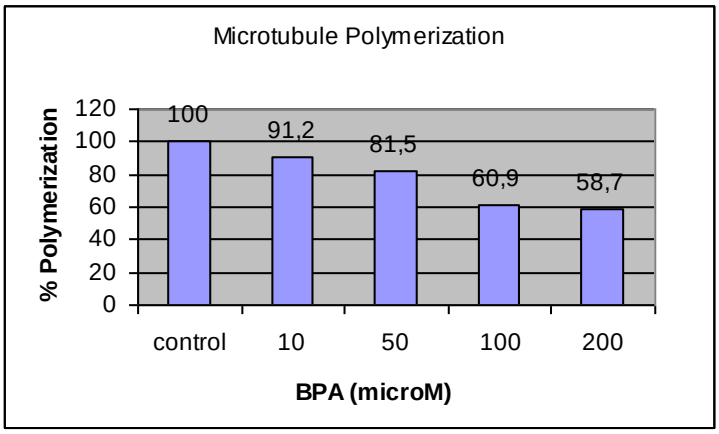

Figure 3.5. Dose-response graph of inhibition of microtubule polymerization caused by BPA.

In the experiments with spTb, SDS-PAGE showed the decrease in the density of pellet fractions and the increase in the density of supernatant fractions in the presence of 200 μM BPA indicating inhibition of microtubule polymerization (Figure 3.6).

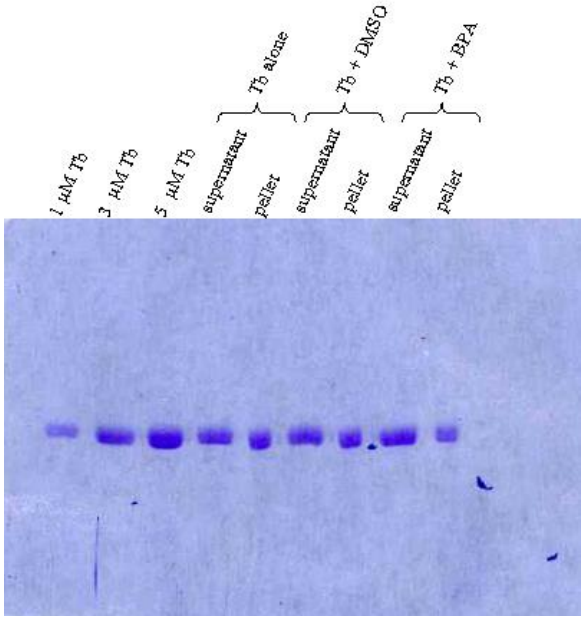

Figure 3.6. SDS-polyacrylamide gel of 5 μM spTb with or without 200 μM BPA.

During the sedimentation experiments with spTb, GTP was not used; since MAPs already facilitate microtubule assembly and stabilizes assembled microtubules. In i*n vitro* conditions, GTP is not needed in the case of MAP-assembled microtubules, but purified tubulin proteins are separated from MAPs; therefore, GTP is needed to facilitate the polymerization of microtubules at 37°C *in vitro*.

BPA was dissolved in DMSO, so additional control experiments were carried out with DMSO. DMSO also showed some inhibitory effects on microtubule polymerization compared to the control reactions. But with 200 μM BPA, inhibition of polymerization was more significant compared to control and DMSO reactions. These suggest that BPA effects are dependent on its accumulation, hence BPA shows its effects in a dose-dependent manner.

To investigate the effects of BPA on polymerized microtubules, we stabilized microtubules with taxol (taxol-stabilized microtubules - TMTs). TMTs were prepared as following: tubulin proteins (10 μM final concentration) were put in 100 μl AB buffer containing 1 mM GTP and 100 μM taxol, and then incubated at 37 °C for 30 minutes. In the sedimentation assay, the final concentration of TMTs was 5 μM in the AB buffer containing 200 μM BPA. Control reactions were performed without BPA. The reaction tubes were incubated either at room temperature (RT) or at 37 °C for 30 minutes. After incubation, the tubes were centrifuged at 127,960 x g (50,000 rpm), at 37 °C for 30 minutes with Beckman Optima Max Ultracentrifuge. Supernatants and pellets were separated and samples were prepared for SDS-PAGE as mentioned before. Then, the fractions on the gel were analyzed quantitatively with Gel Documentation System. TMTs were prepared from either semipurified or purified tubulins.

The results showed that BPA depolymerized assembled microtubules at 37 °C, but not at RT. These are indicated by the decrease in the density of pellet fractions and the increase in the density of supernatant fractions in BPA-treated reactions compared to control reactions (Figure 3.7).

However, the depolymerization effects that were obtained were not as significant with pTb or purified TMTs. In the experiments with pTb, SDS-polyacrylamide gels showed that the density of the pellet fractions of BPA-treated reaction is lower than the pellet of the control reaction (Figure 3.8).

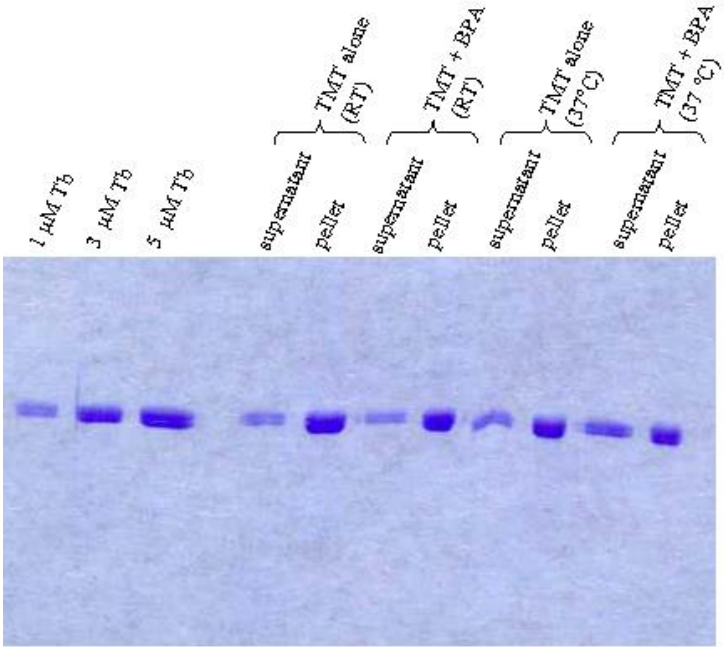

Figure 3.7. SDS-polyacrylamide gel of semi-purified TMT with or without BPA at RT and

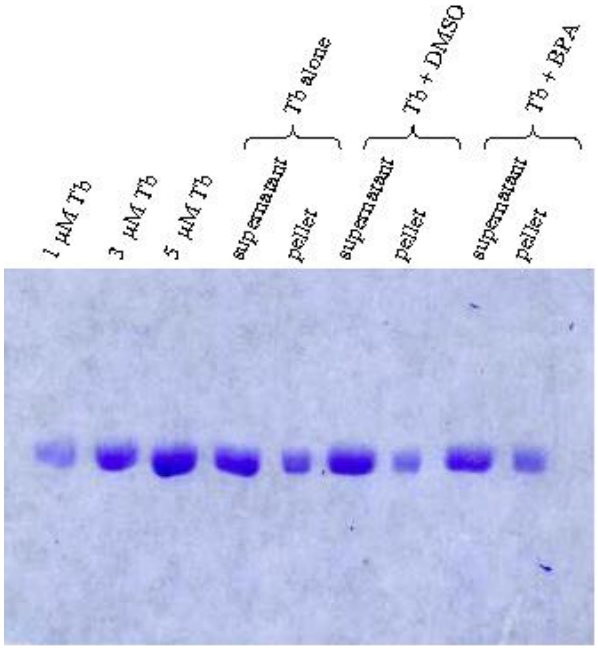

Figure 3.8. SDS-polyacrylamide gel of 5 μM pTb with or without 200 μM

Also, SDS-PAGE of purified TMTs did not show significant difference between BPA-treated and control reactions (Figure 3.9). These result may suggest that BPA shows its effect through MAPs.

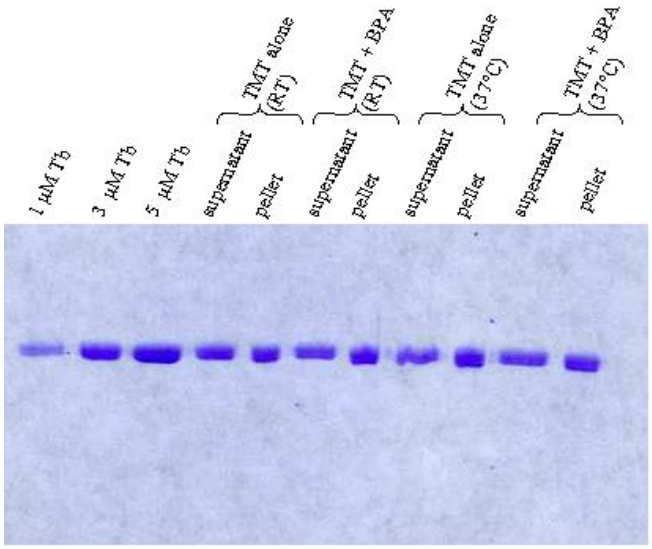

Figure 3.9. SDS-polyacrylamide gel of purified TMTs with or without BPA at RT and

3.3. Fluorescence Spectrometry Results

Luminiscence is the emission of photons from electronically excited states. Fluorescence is the emission which results from the return to the lower orbital of the paired electron. Fluorescence data are generally presented as emission spectra. An emission spectrum is the wavelength distribution of the emission, measured with a single constant excitation wavelength. Such spectra can be presented on either a wavelength scale or a wave number scale. The usual units for wavelength are nanometers, and wave numbers are given in cm^{-1}. An excitation spectrum is the dependence of emission intensity at a single wavelength, upon the excitation wavelength. Briefly, the emission spectra represent the photon flux emitted at each wavelength and the excitation spectra represent the relative quantum yields at excitation wavelength. Corrected spectra are needed for calculation of quantum yields and overlap integrals.

The emission spectra vary widely and are dependent upon the chemical structure of the fluorophore and the solvent in which it is dissolved. Also solvent effects, solvent

relaxation, quenching and a variety of excited state reactions can influence the fluorescence emission.

Fluorescence quenching refers to any process which decreases the fluorescence intensity of a given substance. If a given solvent is very viscous, then the diffusion is slow and the quenching is inhibited.

Fluorescence methods are useful tools for studying the structure and dynamics of living systems, proteins, membranes and their interactions with other macromolecules. A variety of biological molecules contain naturally occurring or intrinsic probes or fluorophores.

Tryptophan is the most highly fluorescent amino acid in proteins. The tryptophan residues of proteins generally account for about 90% of the total fluorescence from proteins. This natural fluorophore is highly sensitive to the polarity of its surrounding environment. Tryptophan appears to be sensitive to quenching by a variety of substances and this sensitivity allows determination of the accessibility of the tryptophan residues in proteins by quenching measurements. Upon excitation at 295 nm, only tryptophan fluorescence is seen.

Tubulin dimers in microtubules contain eight tryptophan residues. The tryptophans are arranged linearly along the long axis of the dimer within 2 nm distance of each other. The indole nucleus of these residues is a uniquely sensitive and complicated fluorophore. Changes in the fluorescence of tryptophan residues can be used to monitor structural transitions by a fluorescence spectrometer. When microtubules are depolymerized to tubulin monomers, tryptophan residues are exposed to the aqueous solvent. Because when depolymerization occurs, tryptophan residues in tubulin dimers become free in the solution, and then, they transfer their energy by vibrating in the environment; hence, the emission spectrum decreases. However, polymerization of tubulin dimers causes stabilization of tryptophan amino acids in the polymer and tryptophan residues fluoresce. This structural transition results in the increased emission spectrum. Tryptophan gives maximum emission intensity at 336 nm when excited at 295 nm.

We compared fluorescence intensities of tryptophan residues of tubulin either in the presence or in the absence of BPA to determine the effect of BPA on microtubule polymerization.

In this experiment, either purified or semi-purified tubulin proteins were used. The final concentration of tubulin proteins was 10 μM in AB buffer containing 1 mM GTP and 200 μM BPA. Control reactions were performed without BPA. Samples were first excited at 295 nm. Variation in the fluorescence spectra and emission intensity of the tryptophan residues in tubulin were monitored at 336 nm as a function of polymerization. The measurements were performed per 2 minutes during 1 hour incubation at 37° C.

In the experiments with semi-purified tubulin, BPA caused an increase in the scattered light indicating microtubule depolymerization (Figure 3.10).

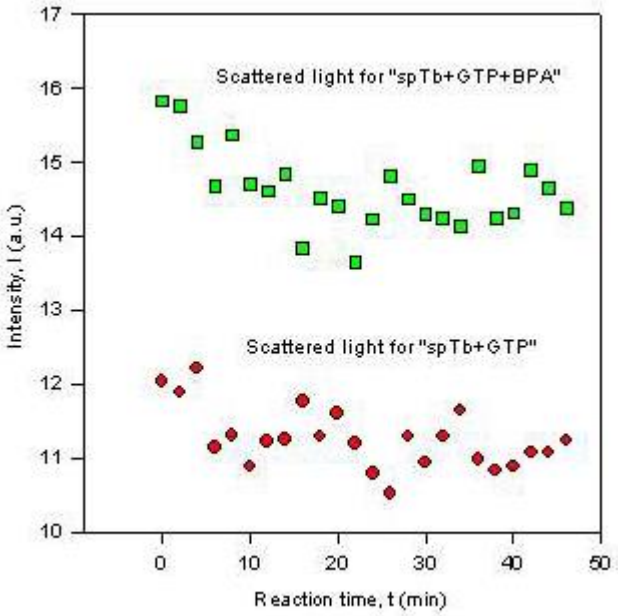

Figure 3.10. Comparison of scattered light values of control and BPA-treated semi-purified tubulins.

Corrected emission intensities which were calculated according to the division of emission intensity to the scattered light degree showed a decrease in the presence of BPA which is correlated with the depolymerization of microtubules (Figure 3.11).

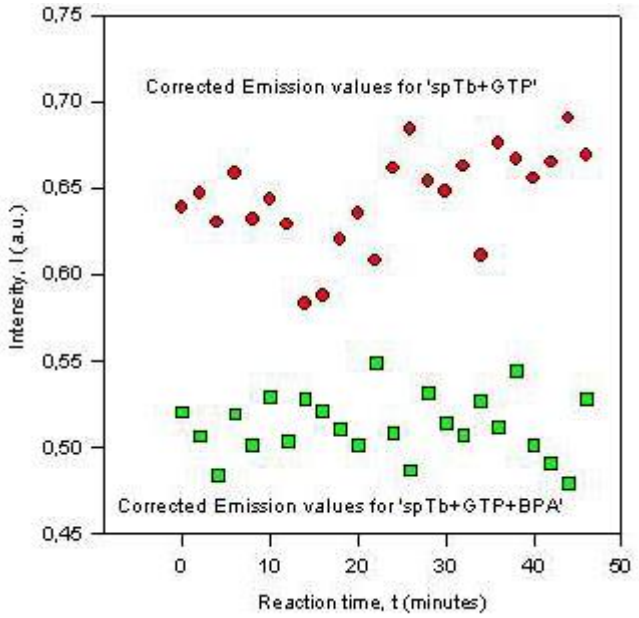

Figure 3.11. Comparison of corrected emission spectra of control and BPA-treated semi-purified tubulins.

A decrease in the emission spectrum is expected when microtubules are depolymerized. In contrast to emission spectrum, scattered light should increase during depolymerization. Either viscosity or turbidity of the environment affects the emission spectrum primarily. These factors increase the emission intensity. During microtubule polymerization, both viscosity and turbidity of the solution increases; hence, the emission spectrum increases. Corrected emission spectrum was calculated by dividing the emission intenstiy to the scattered light degree. Corrected spectrum values were decreased in BPA-exposed reactions compared to the control reactions suggesting the inhibition of microtubule polymerization.

Since the results of sedimentation assays suggested the effect of BPA through MAPs, in the fluorescence spectroscopy experiments with pTb, MAPs were added into the reaction mix at a certain time point. Figure 3.12 shows the comparison of corrected emission spectra between the control and BPA-treated reactions in the presence of MAPs. Corrected emission spectrum values were decreased in the presence of BPA and this indicates the inhibition of microtubule polymerization. This result also suggests that BPA shows its effect through MAPs.

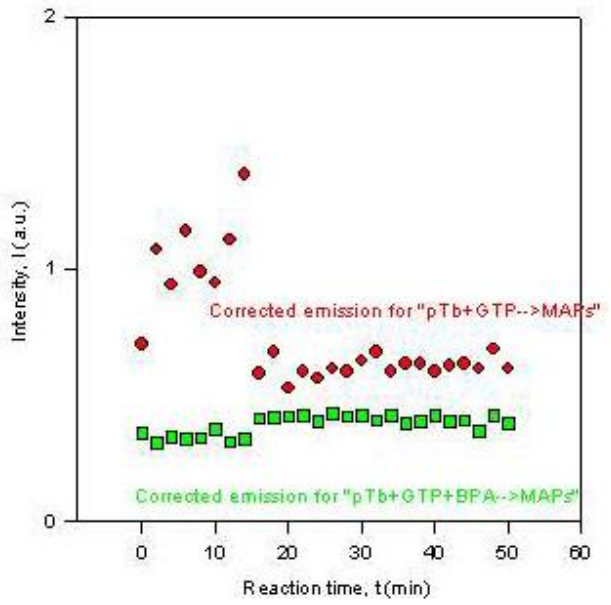

Figure 3.12. Comparison of corrected emission spectra of control and BPA-treated purified tubulin in the presence of MAPs.

3.4. Electron Microscopy Results

Electron microscope allows us to determine the internal structure of both biological and non-biological samples. The principle of transmission electron microscopy (TEM) is based on the transmission of electron beam through the specimen. The darker areas of the image represent those areas of samples that fewer electrons were transmitted through (they are thicker or denser). The lighter areas of the image represent those areas of the sample that more electrons were transmitted through (they are thinner or less dense).

To visualize the morphology of microtubules and the changes in the structure of microtubules when treated with BPA and support the results that we gained with in vitro experiments, we performed electron microscopy experiments.

In electron microscopy experiments, either semi-purified tubulin proteins or TMTs from semi-purified tubulins were used. 10 μM tubulin or 10 μM TMTs were incubated with 5 mM GTP and 100 μM BPA at 37° C for 1 hour. Control reactions were performed without BPA. After incubation, the tubes were centrifuged with Beckman Optima Max Ultracentrifuge, at 127,960 x g (50,000 rpm), 37° C for 30 minutes. The supernatants were decanded. 20 μl 4% gluteraldehyde was added onto

pellets and left for 15 minutes for fixation. The samples were adsorbed to pioloform coated electron microscope grids by inserting grids into resuspended pellets in the tubes for 20 seconds. Then, grids were washed by plunging into distilled water three times and left for air-dry for 30 minutes and negatively stained with 2% uranyl acetate.

In trial assays, reliable results with semi-purified tubulin could not be obtained. Microtubules are not resistant to harsh conditions such as grid preparation, staining and washing procedures; hence, they could depolymerize.

However, taxol-stabilized microtubules (TMTs) were visualized as long cylindrical structures in control experiments (Figure 3.13). Since taxol stabilizes microtubules, TMTs are may not affected by the preparation steps.

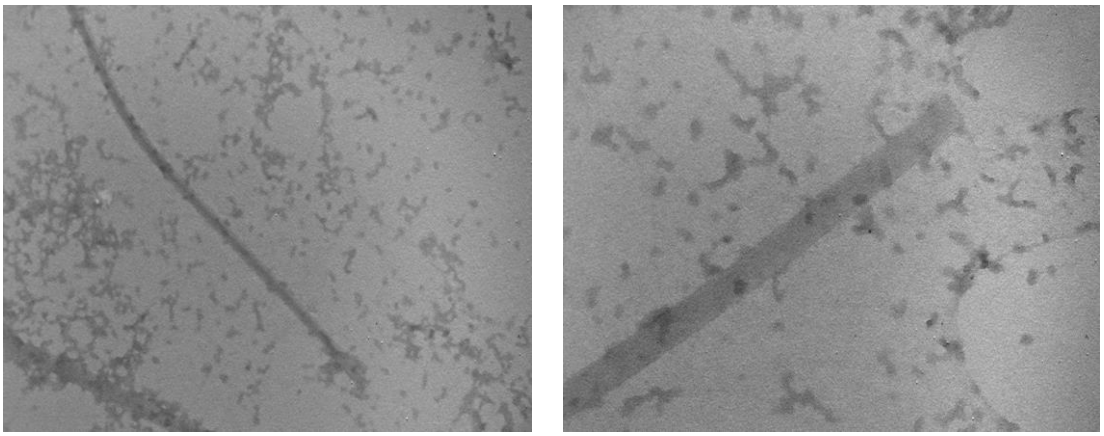

A) **B)**

Figure 3.13. Electron micrographs of taxol-stabilized microtubules (TMTs) (control).
A) 50,000x, B) 100,000x

BPA caused different microtubule structures such as rings or spiral, relaxed structures consistent with depolymerization of microtubule structure and disintegration (Figure 3.14).

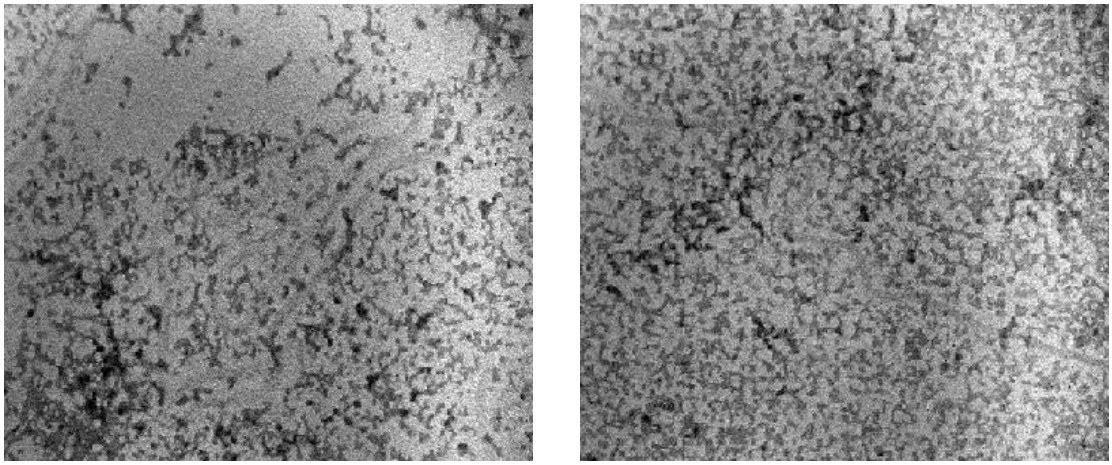

Figure 3.14. Electron micrographs of microtubules when treated with 100 μM BPA (x50,000).

4. CONCLUSIONS

Microtubules are cytoskeletal elements in all eukaryotic cells that are necessary for many functions including intracellular transport, morphogenesis, motility and cell division. In previous studies, BPA has been reported to disrupt the cytoplasmic microtubule complex and mitotic spindle in cultured cells. It induces metaphase arrest and micronuclei containing chromosomes. In addition to its estrogenicity, BPA acts as an aneuploidogen. This potential is possibly based on the interaction with microtubules. Our study indicates that BPA interacts with microtubules and disrupts microtubule formation under cell-free conditions. BPA inhibits microtubule polymerization in a concentration-dependent manner. BPA depolymerizes taxol-stabilized microtubules. BPA causes abnormal microtubule structure such as spiral, relaxed and disintegrated microtubules consistent with depolymerization. The experimental results also suggest that BPA may show its effects on microtubules through microtubule-associated proteins. This needs to be further investigated. Further research involving analysis of effects of BPA on microtubule associated proteins will help to understand the exact molecular mechanism of BPA toxicity.

REFERENCES

[1] **Lodish, H., Berk, A., Zipursky, S.L., Matsudaira, P., Baltimore, D., Darnell, J.E.**, 2000. Molecular Cell Biology (4th edition). W.H. Freeman & Co, New York, USA.

[2] **Furukawa, R., Fechheimer, M.**, 1997. The structure, function, and assembly of actin filament bundles, *Int. Rev. Cytol.*, **175**, 29-90.

[3] **Erickson, H.P.**, 1998. Atomic structures of tubulin and FtsZ, *Trends Cell Biol.*, **8**, 133-137.

[4] **Zigmond, S.H.**, 1998. Actin cytoskeleton: the Arp2/3 complex gets to the point, *Curr. Biol.*, **8**, 654-657.

[5] **Alberts, B., Johnson, A., Lewis, J., Raff, M., Roberts, K., Walter, P.**, 2002. Molecular Biology of the Cell (4th edition). Garland Science, USA.

[6] **McGough, A.**, 1998. F-actin-binding proteins, *Curr. Opin. Struct. Biol*, **8**, 166-76.

[7] **Theriot, J.A.**, 1997. Accelerating on a treadmill: ADF/cofilin promotes rapid actin filament turnover in the dynamic cytoskeleton, *J. Cell Biol.*, **136**, 1165-1168.

[8] **Kwiatkowski, D.J.**, 1999. Functions of gelsolin: motility, signaling, apoptosis, cancer, *Curr. Opin. Cell Biol.*, **11**, 103-108.

[9] **Simmon, R.**, 1996. Molecular motors: single-molecule mechanics, *Curr. Biol.*, **6**, 392-394.

[10] **Rayment, I.**, 1996. The structural basis of the myosin ATPase activity, *J. Biol. Chem.*, **271**, 15850-15853.

[11] **Coluccio, L.**, 1997. Myosin I, *Am. J. Physiol.*, **273**, C347-C359.

[12] **Gregorio, C.C., Granzier, H., Sorimachi, H., Labeit, S.**, 1999. Muscle assembly: a titanic achievement?, *Curr. Opin. Cell Biol.*, **11**, 18-25.

[13] **Squire, J.M., Morris, E.P.**, 1998. A new look at thin filament regulation in vertebrate skeletal muscle, *FASEB J.*, **12**, 761-771.

[14] **Field, C., Li, R., Oegema, K.**, 1999. Cytokinesis in eukaryotes: a mechanistic comparison, *Curr. Opin. Cell Biol.*, **11**, 68-80.

[15] **Desai, A., Mitchison, T.J.**, 1997. Microtubule polymerization dynamics, *Annu. Rev. Cell Dev. Biol.*, **13**, 83-117.

[16] **Nogales, E., Wolf, S.G., Downing, K.H.**, 1998. Structure of the alpha beta tubulin dimer by electron crystallography, *Nature*, **391**, 199-203.

[17] **Nogales, E.**, 2001. Structural insight into microtubule function, *Annu. Rev. Biophys. Biomol. Struct.*, **30**, 397-420.

[18] **Mitchison, T., Kirschner, M.**, 1984. Dynamic instability of microtubule growth, *Nature*, **312**, 237-242.

[19] **Vaughn, K.C., Harper, J.D.I.**, 1998. Microtubule-organizing centers and nucleating sites in land plants, *Int. Rev. Cytol.*, **181**, 75-149.

[20] **Baas, P.W.**, 1996. The neuronal centrosome as a generator of microtubules for the axon, *Curr. Topics Dev. Biol.*, **33**, 281-298.

[21] **Erickson, H.P., O'Brien, E.T.**, 1992. Microtubule dynamic instability and GTP hydrolysis, *Annu. Rev. Biophys. Biomol. Struct.*, **21**, 145-166.

[22] **Maccioni, R.B., Cambiazo, V.**, 1995. Role of microtubuleassociated proteins in the control of microtubule assembly, *Physiol. Rev.*, **75**, 835-864.

[23] **Mandelkow, E., Mandelkow, E.M.**, 1995. Microtubules and microtubule-associated proteins, *Curr. Opin. Cell Biol.*, **7**, 72-81.

[24] **Goodson, H.V., Valetti, C., Kreis, T.E.**, 1997. Motors and membrane traffic, *Curr. Opin. Cell Biol.*, **9**, 18-28.

[25] **Thaler, C.D., Haimo, L.T.**, 1996. Microtubules and microtubule motors: mechanisms of regulation, *Int. Rev. Cytol.*, **164**, 269-327.

[26] **Mandelkow, E., Johnson, K.A.**, 1998. The structural and mechanochemical cycle of kinesin, *Trends Biochem. Sci.*, **23**, 429-433.

[27] **Hirokawa, N.**, 1998. Kinesin and dynein superfamily proteins and the mechanism of organelle transport, *Science*, **279**, 519-526.

[28] **Moore, J.D., Endow, S.A.**, 1996. Kinesin proteins: a phylum of motors for microtubule-based motility, *Bioessays*, **18**, 207-219.

[29] **Holleran, E.A., Karki, S., Holzbaur, E.L.F.**, 1998. The role of the dynactin complex in intracellular motility, *Int. Rev. Cytol.*, **182**, 69-109.

[30] **Inoue, S.**, 1996. Mitotic organization and force generation by assembly/disassembly of microtubules, *Cell Struc. Funct.*, **21**, 375-379.

[31] **Nicklas, R.B.**, 1997. How cells get the right chromosomes, *Science*, **275**, 632-637.

[32] **Saunders, W.S.**, 1999. Action at the ends of microtubules, *Curr. Opin. Cell Biol.*, **11**, 129-133.

[33] **Downing, K.H.**, 2000. Structural basis for the interaction of tubulin with proteins and drugs that affect microtubule dynamics, *Annu. Rev. Cell Dev. Biol.*, **16**, 89-111.

[34] **Ben-Jonathan, N., Steinmetz, R.**, 1998. Xenoestrogens: The Emerging Story of Bisphenol A, *TEM*, **9,** 124-129.

[35] **Pfeiffer, E., Rosenberg, B., Deuschel, S., Metzler, M.**, 1997. Interference with microtubules and induction of micronuclei in vitro by various bisphenols, *Mutation Research*, **390**, 21-31.

[36] **Staples, C.A., Dorn, P.B., Klecka, G.M., O'Block, S.T., Harris, L.R.**, 1998. A Review of the Environmental Fate, Effects, and Exposures of Bisphenol A, *Chemosphere*, **36**, 2149-2173.

[37] **Rivas, A., Lacroix, M., Olea-Serrano, F., Laios, I., Leclercq, G., Olea, N.**, 2002. Estrogenic effect of a series of bisphenol analogues on gene and protein expression in MCF-7 breast cancer cells, *Journal of Steroid Biochemistry & Molecular Biology*, **82**, 45-53.

[38] **Kamrin, M.A.**, 2004. Bisphenol A: A Scientific Evaluation, *Medscape General Medicine*, **6(3)**, 10-18.

[39] **Sonnenschein, C., Soto, A.M.**, 1998. An Updated Review of Environmental Estrogen and Androgen Mimics and Antagonists, *J. Steroid Biochem. Molec. Biol.*, **65**, 1-6.

[40] **Farabollini, F., Porrini, S., Dessi-Fulgheri, F.**, 1999. Perinatal Exposure to the Estrogenic Pollutant Bisphenol A Affects Behavior in Male and Female Rats, *Pharmacology Biochemistry and Behavior*, **64**, 687-694.

[41] **Witorsch, R.J.**, 2002. Low-dose in utero effects of xenoestrogens in mice and their relevance to humans: an analytical review of the literature, *Food and Chemical Toxicology*, **40**, 905-912.

[42] **Roy, D., Colerangle, J.B., Singh, K.P.**, 1998. Is Exposure to Environmental or Industrial Endocrine-Disrupting Chemicals Able to Cause Genomic Instability?, *Frontiers in Bioscience*, **3**, 913-921.

[43] **Iida, H., Maehara, K., Doiguchi, M., Mori, T., Yamada, F.**, 2003. Bisphenol A-induced apoptosis of cultured rat Sertoli cells, *Reproductive Toxicology*, **17**, 457-464.

[44] **Suzukia, A., Sugiharaa, A., Uchidab, K., Satoa, T., Ohtac, Y., Katsub, Y.**, 2002. Developmental effects of perinatal exposure to bisphenol-A and diethylstilbestrol on reproductive organs in female mice, *Reproductive Toxicology*, **16**, 107-116.

[45] **Markey, C.M., Rubin, B.S., Soto, A.M., Sonnenschein, C.**, 2003. Endocrine disruptors: from Wingspread to environmental developmental biology, *Journal of Steroid Biochemistry & Molecular Biology*, **83**, 235-244.

[46] **Kabuto, H., Amakawa, M., Shishibori, T.**, 2004. Exposure to bisphenol A during embryonic/fetal life and infancy increases oxidative injury and causes underdevelopment of the brain and testis in mice, *Life Sciences*, **74**, 2931-2940.

[47] **European Commission Directorate – General Health and Consumer Protection**, 2002. Bisphenol A: Human Health Part, *31th CSTEE (Scientific Committee on Toxicity, Ecotoxicity and the Environment) plenary meeting*, Brussels, May 22.

[48] **Ochi, T.**, 1999. Induction of multiple microtubule-organizing centers, multipolar spindles and multipolar division in cultured V79 cells exposed to diethylstilbestrol, estradiol-17b and bisphenol A, *Mutation Research*, **431**, 105-121.

[49] **Tsutsumi, O.**, 2005. Assessment of human contamination of estrogenic endocrine-disrupting chemicals and their risk for human reproduction, *Journal of Steroid Biochemistry & Molecular Biology*, **Article in Press**.

[50] **Wistuba, J., Brinkworth, M.H., Schlatt, S., Chahoud, I., Nieschlag, E.**, 2003. Intrauterine bisphenol A exposure leads to stimulatory effects on Sertoli cell number in rats, *Environmental Research*, **91**, 95-103.

[51] **Kim, J.C., Shin, H.C., Cha, S.W., Koh, W.S., Chung, M.K., Han, S.S.**, 2001. Evaluation of developmental toxicity in rats exposed to the environmental estrogen

bisphenol A during pregnancy, *Life Sciences*, **69**, 2611-2625.

[52] **Chun, T.Y., Gorski, J.**, 2000. High Concentrations of Bisphenol A Induce Cell Growth and Prolactin Secretion in an Estrogen-Responsive Pituitary Tumor Cell Line, *Toxicology and Applied Pharmacology*, **162**, 161-165.

[53] **Oka, T., Adati, N., Shinkai, T., Sakuma, K., Nishimura, T., Kurosee, K.**, 2003. Bisphenol A induces apoptosis in central neural cells during early development of *Xenopus laevis*, *Biochemical and Biophysical Research Communications*, **312**, 877-882.

[54] **Suzukia, N., Hattori, A.**, 2003. Bisphenol A suppresses osteoclastic and osteoblastic activities in the cultured scales of goldfish, *Life Sciences*, **73**, 2237-2247.

[55] **Katoha, K., Matsudaa, A., Ishigamia, A., Yonekuraa, S., Ishiwataa, H., Chena, H., Obaraa, Y.**, 2004. Suppressing effects of bisphenol A on the secretory function of ovine anterior pituitary cells, *Cell Biology International*, **28**, 463-469.

[56] **Negishia, T., Ishiia, Y., Kyuwaa, S., Kurodab, Y., Yoshikawa, Y.**, 2003. Inhibition of staurosporine-induced neuronal cell death by bisphenol A and nonylphenol in primary cultured rat hippocampal and cortical neurons, *Neuroscience Letters*, **353**, 99-102.

[57] **Funabashi, T., Kawaguchi, M., Furuta, M., Fukushima, A., Kimura, F.**, 2004. Exposure to bisphenol A during gestation and lactation causes loss of sex difference in corticotropin-releasing hormone-immunoreactive neurons in the bed nucleus of the stria terminalis of rats, *Psychoneuroendocrinology*, **29**, 475-485.

[58] **Masuoa, Y., Moritab, M., Okac, S., Ishido, M.**, 2004. Motor hyperactivity caused by a deficit in dopaminergic neurons and the effects of endocrine disruptors: a study inspired by the physiological roles of PACAP in the brain, *Regulatory Peptides*, **123**, 225-234.

[59] **Aoua, S., Inouea, T., Fujimotoa, T., Mizunoa, M., Oomurab, Y., Kubob, K., Arai, O.**, 2004. Chemical impacts on higher brain functions, *International Congress Series*, **1269**, 101-104.

[60] **Sugita-Konishi, Y., Shimura, S., Nishikawa, T., Sunaga, F., Naito, H., Suzuki, Y.**, 2003. Effect of Bisphenol A on non-specific immunodefenses against non-pathogenic *Escherichia coli*, *Toxicology Letters*, **136**, 217-227.

[61] **Byuna, J.A., Heob, Y., Kimc, Y.O., Pyoa, M.Y.**, 2005. Bisphenol A-induced downregulation of murine macrophage activities in vitro and ex vivo, *Environmental Toxicology and Pharmacology*, **19**, 19-24.

[62] **Takahashi, S., Chi, X.J., Yamaguchi, Y., Suzuki, H.**, 2001. Mutagenicity of bisphenol A and its suppression by interferon-a in human RSa cells, *Mutation Research*, **490**, 199-207.

[63] **Haighton, L.A., Hlywka, J.J., Doull, J.**, 2002. An Evaluation of the Possible Carcinogenicity of Bisphenol A to Humans, *Regulatory Toxicology and Pharmacology*, **35**, 238-254.

[64] **Kabuto, H., Hasuike, S., Minagawa, N., Shishibori, T.**, 2003. Effects of bisphenol A on the metabolisms of active oxygen species in mouse tissues, *Environmental Research*, **93**, 31-35.

[65] **Metzler, M., Pfeiffer, E.**, 1995. Effects of Estrogens on Microtubule Polymerization in Vitro: Correlation with Estrogenicity, *Environmental Health Perspectives*, **103**, 21-22.

[66] **Nakagomi, M., Suzuki, E., Usumi, K., Saitoh, Y.**, 2001. Effects of Endocrine Disrupting Chemicals on the Microtubule Network in Chinese Hamster V79 Cells in Culture and in Sertoli Cells in Rats, *Teratogenesis, Carcinogenesis, and Mutagenesis*, **21**, 453-462.

[67] **Lehmann, L., Metzler, M.**, 2004. Bisphenol A and its methylated congeners inhibit growth and interfere with microtubules in human fibroblasts in vitro, *Chemico-Biological Interactions*, **147**, 273-285.

[68] **Hunt, P.A., Koehler, K.E., Susiarjo, M., Hodges, C.A.**, 2003. Bisphenol A Exposure Causes Meiotic Aneuploidy in the Female Mouse, *Current Biology*, **13**, 546-553.

RESUME

Eyser KILIÇ was born in ISTANBUL in 1981. After getting her high school diploma from 50. Year İnsa High School in 1998 and at the same year, she started her undergraduate degree in Istanbul University, Cerrahpaşa Medical Faculty, Department of Biomedical Sciences. She had her Bachelor's degree in 2002. She was accepted to Istanbul Technical University, Advanced Technologies in Engineering, Molecular Biology-Genetics and Biotechnology program in 2002. She has been also working as a research assistant in Department of Molecular Biology and Genetics. She is still pursuing her studies in the same department.